PREPARATION CHARACTERIZATION AND SINTERING OF SOL - GEL PROCESSED ZIRCONIA COATINGS

A Thesis Submitted

in Partial Fulfilment of the Requirements

for the Degree of

MASTER OF TECHNOLOGY

by

V. V. S. N. N. CHAKRAPANI

to the

MATERIALS SCIENCE PROGRAMME

INDIAN INSTITUTE OF TECHNOLOGY KANPUR

December 1989

To My Beloved Father...

CERTIFICATE

This is to certify that this work on "PREPARATION, CHARACTERIZATION AND SINTERING OF SOL-GEL PROCESSED ZIRCONIA COATINGS" by V.V.S.N.N. Chakrapani has been carried out under my supervision and that this has not been submitted elsewhere for any degree.

(D.C. Agrawal)
Professor
Materials Science Programme
Indian Institute of Technology
Kanpur 208016

ACKNOWLEDGEMENTS

I would like to express my deep gratitude to Dr. D.C. Agrawal for his valuable guidance through out this work. I sincerely thank him for introducing me to this field and for his forbearance in many occassions. I thank him also for doing the profilometer measurements at Cornell University, USA.

I thank Dr. T. Rajagopalan for helping me in the SEM studies.

I thank Dr. T.K. Chandrasekhar for allowing me to use the spectrophotometer.

I thank all of the non-teaching staff of ACMS for their cooperation during this work especially Mr. Uma Shankar, Mr. Jain and Sharma. I thank Mr. Jain for his neat drafting work.

My special thanks are due to friends Agni, Sanjay, Rekha, Sudhakar, DP, Appu who have given me moral support and encouragement throughout this work.

I thank all of my lab-mates and friends who have been very much cooperative during my stay at I.I.T. Kanpur.

I also thank Mr. U.S. Mishra for his neat typing work.

V.V.S.N.N. Chakrapani

CONTENTS

LIST OF TABLES

LIST OF FIGURES

ABSTRACT

Coatings of zirconia on sapphire ($11\bar{2}0$) single crystals were formed by dip coating from the sol of zirconium-n-propoxide, DEA, isopropanol and water. The thickness of the coatings as determined by interferometry was varied between 40 and 140 nm by multiple dipping with intermediate drying steps at 50°C. The as deposited coatings were amorphous and changed to cubic and monoclinic phases after heating to 450°C and 900°C respectively. The phase transformation route was amorphous - cubic – tetragonal – monoclinic in the case of powders prepared from the same sol as used for coating. Heating of the coatings at 1250°C resulted in breakup of the coating and development of porosity because of a relatively high contact angle between sapphire and zirconia. The development of porosity is delayed as the coating thickness is increased. The porosity increases with annealing time and approaches a constant value which corresponds to the formation of well separated islands of the coating. The grain size also increases with the annealing time, slowly at first and then at a steeper rate due to the exaggerated grain growth. The wetting of ZrO_2 on glass slides is better than that on sapphire. The optical band gap energy of the films was found to be 5.498 eV. The doping of ZrO_2 powder with 8 mole% Y_2O_3 has stabilized tetragonal phase.

CHAPTER I

INTRODUCTION

Ceramic coatings are used in a variety of applications such as optical, thermal barrier, sensors etc. Conventional ceramic coatings were largely limited to corrosion prevention and decorative enhancement, but the new technologies offer a far wider range of benefits. The emphasis of today's 'Research' is on the development of a variety of ceramic coatings for diverse applications. One of such new promising technologies developed in the recent years is the sol-gel technology. Ceramic coated metals are used for furnace components, heat treating equipment, chemical processing equipment, heat exchangers, socket motor nozzles,exhaust manifolds,jet engine parts and nuclear power plant components etc. The other modern applications of ceramic coatings obtained through sol-gel processes include antireflection coatings on glass picture frames, instrument cover glasses and monitor screens for computers and television sets, and many more.

I.1 Ceramic Coatings

Ceramic coatings refer to coatings of oxides carbides, silicides, borides, nitrides, cermets and the super percelains and other inorganic materials.

I.1.a **Coating Methods**

Ceramic coatings are formed by the following methods[1]:

1. Spraying
2. Dipping
3. Flow coating
4. Combustion flame spraying
5. Plasma-arc flame spraying
6. Detonation gun spraying
7. Pack cementation
8. Fluidized bed deposition
9. Vapour streaming (or CVD)
10. Electrophorosis
11. Ion assisted electron beam deposition[2]
12. Sol-gel processing (explained in detail with ZrO_2 as an example)

I.1.a.1 **Spraying and Dipping**

Spraying and dipping are two methods of applying ceramic coatings in a slip or slurry form. Spraying and dipping methods are used to apply coatings onto engine exhaust dusts, space heaters, radiators, and other high production parts. Spraying can be used when the shape of the work permits direct access to all surface areas to be coated. Dipping can be used for almost all parts.

I.1.a.2 **Flow Coatings**

Flow coating is modified dipping and draining in which slip is flowed onto conveyorized parts. Slip flows from nozzles, designed to flush all surfaces of the work, after which it

drains into a catch basin and is recirculated.

I.1.a.3 **Flame Spraying**

Most ceramic coating materials used currently can be applied by flame spraying. This method involves heating and propelling the particles in the plastic condition to the substrate surface. Three types are as follows:

a) Combustion flame spraying
b) Plasma arc spraying
c) Detonation gun spraying.

The first two methods usecoating materials in powder or rod form. Detonation gun spraying uses only powder materials.

a) Combustion Flame Spraying

The processing variables of flame spraying that affect the serviceability of a coating are:

i) Surface preparation
ii) Gun operation
iii) Spraying distance
iv) Temperature of the work piece
v) Type of coating.

b) Plasma Arc Spraying

In this process, a gas or a mixture of gases, such as argon, hydrogen, or nitrogen is fed into the arc chamber of the plasma generator and heated by an electric arc struck between an electrode and the nozzle. The gas is heated to temperatures as high as 8300^{o}C to form a plasma, or ionized gas, that is

accelerated through the nozzle. The ceramic powder, carried by a gas stream, is injected into the plasma where it is heated, melted, and propelled towards the workpiece.

c) Detonation Gun Spraying

It uses controlled detonations of acetylene and oxygen to melt and propel the particles onto the substrate.

I.1.a.4 **Cementation Process**

Pack cementation, the fluidized bed process, and vapor streaming are three types of cementation processes used in ceramic coating. These methods provide impervious, oxidation protection coatings.

a) **Fluidized Bed Cementation Processes**

This process for applying ceramic coatings involves

1) Thermal decomposition and displacement reactions of metal halides.

2) Presence of hydrogen to reduce the halides.

3) Diffusion of deposited materials into the substrate metal to produce an intermetallic compound.

b) **Vapor Streaming Cementation**

Vapor streaming is a cementation process in which a vapor of the coating material is decomposed on the surface of a heated part.

I.1.a.5 **Electrophoresis**

Electrophoresis is the migration of electrically charged

particles suspended in a colloidal solution under the influence of an applied electric field. Deposition occurs at one of the electrodes where the charge on the particles is neutralized. The particles acquire a static charge during milling, or they can be charged artificially by absorption of certain additives or electrolytes.

I.1.b **Significance of ZrO_2 Coatings**

Thermal barrier coatings are under active development to increase the high temperature capability of gas turbines blades and vanes. These are currently used on combustion chambers and their use for turbine components is limited by their poor thermal shock resistance. Large effort is currenly being expended in developing these coatings with increased fracture resistance and thereby high reliability. Most of these investigations pertain to ZrO_2 based ceramics as they have the lowest thermal conductivity and are highly thermal shock resistant[3]. Reliable phase diagrams and other thermophysical data are available for ZrO_2 based systems to aid the developmental effort. ZrO_2 undergoes polymorphic transformation and the cubic phase can be stabilized by addition of divalent and trivalent cations like Ca, Mg and Y. Thus ZrO_2 based coatings can be formed with different phases covering a wide range of properties.

ZrO_2 coatings on carbon-carbon composites provide protection against oxidation[4]. Useful oxidation resistance upto 1000°C can be obtained by ZrO_2 coatings. Composite coatings composed of ZrO_2 and SiC Whiskers[5] enhance the performance of oxidation resistant coatings.

ZrO_2 films have high dielectric constant ~ 18 and greater impermeability to impurity diffusion[6]. They are used as insulating layers in multilayer electronic devices. ZrO_2 film has a potential use for storage capacitor in the dynamic random access memory. ZrO_2 crystal is an interesting material for insulating layers in silicon-on-insulator devices because the pure or stabilized oxide can be closely matched in lattice constant to silicon. Low loss ZrO_2 films for optical applications in the UV region are discussed by Apparao et al[7].

The multicomponent oxide layers having ZrO_2 as one of the constituents have very good alkali resistance and improved chemical durability. ZrO_2 coatings can also be applied onto the glass bodies to fill in the microflows and thereby increase the strength of the glass. Charge storage in anodic ZrO_2 films[8],and oxygen sensor elements having thin layer of stabilized ZrO_2 sintered on a substrate[9] are also in use.

Varieties of methods of coating ZrO_2 are in practice. ZrO_2 and stabilized ZrO_2 films were prepared by Kamata et al[10] by chemical vapour deposition using hydrolysis of β-diketone chelates such as Zr $(C_{11}\ H_{19}\ O_2)_4$. Spray pyrolysis[11] of n-butyl zirconate deposited adherent, transparent ZrO_2 coatings on glass and Alumiium substrates. Abrasion resistance of Aluminium substrates was enhanced as a result of this.

The ZrO_2 films obtained by electron-beam evaporation were characterized by Krivosheer et al for structrure and optical properties[12]. Substantial packing density resulting in refractive indices close to the bulk values are obtained in ZrO_2 films by ion assisted electron beam deposition[13]. Patent-ZrO_2 based coatings by hot isostatic compaction was given

by Rolls-Royce Ltd.[14]. Composition, structure and conductivity of rf sputtered calcia stabilized zirconia thin films was dealt by Michel Croset et al[15]. Plasma arc spraying method is extensively studied for the deposition of ZrO_2 layers. Mechanical and physical properties of the plasma sprayed, stabilized ZrO_2 are dealt[16] by Siemens. Phase distribution in plasma sprayed ZrO_2-Y_2O_3 is studied by Miller et al[17,18]. A plenty of literature is available for plasma sprayed ZrO_2 coatings on various aspects[19,20,21,22,23,24]. Low temperature preparation of stabilized ZrO_2 films is done by Dongare et al[25]. The thermal decomposition of the alkoxide at 400°C gives a ZrO_2 coating which is purely on oxygen ion conductor.

The anodic ZrO_2 films obtained by Panagopoulos[26] were cubic for thickness < 100 nm and with a mixture of cubic and tetragonal for thicker films. ZrO_2 thin films deposited by laser assisted evaporation[27] on room temperature substrates had crystalline oriented structures. Low optical absorption and high refractive index values indicated the stoichiometric and dense nature of these films. Fukumoto et al[28] observed the growth characteristics of the vacuum evaporated crystalline films of ZrO_2. The crystalline system of ZrO_2 films depends on substrate temperature. The chemical vapour deposition and characterization of ZrO_2 films from organometallic compounds by CVD is done by Balog et al[6]. The sol-gel derived ZrO_2 coatings are treated separately under the literature survey section. The sol-gel processing of ZrO_2 coatings is yet to be developed to compete with the other processing methods. The basic understanding of the film formation and structure

stabilization of ZrO_2 is necessary to produce useful coatings by sol-gel method.

I.2 Sol-Gel Processes

All sol-gel processes start with a sol which undergoes a transformation to give rise to a gel. A sol can be defined as a suspension of submicron particles in suspension in a liquid. These particles can be fine powders or even small molecules as in a sol of metallo-organic compounds in alcohol. The colloidal sols formed by the suspension of submicron particles in aqueous medium are physical sols and the processes with those solutions are physical sol-gel processes. The second one is a different class of sol wherein chemical reactions take place to give rise to an oxide network. These are chemical sol-gel processes. "The sol-gel process in general is the name applied to any one of a number of processes that involve a sol that undergoes a sol-gel transition"[29]. After the transition the sol becomes a rigid, porous mass, known as a gel. A true one phase sol goes through a sol-gel transition to give rise to a two phase system of solid and solvent filled pores. The oxides are obtained by heat treating these gels. The chemical sol-gel processes are more versatile than the physical sol-gel processes. So only the former one is discussed here.

Sol-gel technology has been developed to prepare metal oxide fibres, monoliths, microspheres, thin films and fine powders etc. These have large number of applications such as, antireflexion coatings, protective coatings, catalysts, piezoelectric devices, waveguides, optical lenses and fibres;

high strength ceramics, speciality glasses, nuclear waste encapsulation and many others.

The oxide coatings produced by sol-gel processing are commercially important as compared to the other products the reason being that only a small amount of material is needed and also it is possible to coat large surface areas. There is a great technological interest to produce multilayered dielectric films through sol-gel process.

The sol-gel processes offer the following advantages over the conventional methods.

1) High purity materials are involved in the process so high purity products are obtained.

2) Mixing takes place in molecular level so we can get molecular level homogeneity in multicomponent materials.

3) Lower processing temperatures hence low energy requirements.

4) Doping and stabilizing ceramic materials is effective.

5) Single, multicomponent oxide; nonoxide ceramics can be processed.

6) The sol-gel products melt to clear glasses or sinter to dense bodies at temperatures considerably lower than the equivalent compositions prepared by classical methods.

7) Simple, and need no high capital investment.

8) Submicron particle size (20-50^{o}A) with narrow range is possible to produce.

9) High reactivity and surface area of the powders obtained by this process allow them to sinter to near theoretical densities.

I.2.a History of Sol-Gel Coatings

The earliest investigations concerning oxide coatings deposited from solutions (sol-gel process) were those of Geffcken and Berger[30] about 50 years ago. They prepared single oxide coatings. Schroeder has developed a thin film physics[31] for this process by using single oxide and mixed oxide layers about 20 years back. The first studies of this kind were stimulated by Langmuir's observation[32] that certain insoluble substances of high molecular weight containing polar groups spread over a water surface as a monomolecular layer, and that such films could be deposited onto planar solid surfaces by slowly draining the water or raising the substrate. In 1935, Blodgett[33] produced antireflection coatings by this method. The first products appeared on the market in 1953. Large scale production of automotive rear-view mirrors (TiO_2-SiO_2-TiO_2)[34] started in 1959, and continued with antireflection coatings (TiO_2/SiO_2-TiO_2-SiO_2) in 1964, and with sun shielding windows (Registered Trade Names CALOREX IROX; essentially TiO_2) in 1969. Many more products are presently manufactured which are dealt separately under 'Applications' Section.

The basic principle of the chemical reactions and process technology for the preparation of dielectrics as films on nonmetallic substrates were known when in 1969 Dislich and Hinz elaborated the chemical basis for preparation of multicomponent oxides. Patent applications were filed in 1969 and were granted in industrial countries. The details of the process were published[35] in 1971.

Since 1971, there has been a lot of research work done

in the field of sol-gel process. It has been known since then, that any type of multicomponent oxide can be synthesized using the alkoxides of various elements by the sol-gel process. Recent developments show that it is possible to synthesize in thin film form glasses, crystals and glass ceramics which are not even easy to fabricate in bulk form. The sol-gel products which are on the market as on 1981[36], 1987[37] are dealt elsewhere. SiO_2-TiO_2[38]; SiO_2-ZrO_2[39,40]; SiO_2-TiO_2-ZrO_2[41], Al_2O_3-P_2O_5[42]; B_2O_3-P_2O_5[42]; CeO_2-TiO_2[43] and many more multioxide coatings have been prepared to meet with different purposes. The chemical reactions, effects of coating techniques, process parameters, effects of additions of external reagents have been studied extensively for the oxide coatings like SiO_2[44,45,31] and TiO_2[46,47,48]. Other oxide coatings like PZT[49], ZrO_2[50], VO_2[51], Ta_2O_5[52] and Al_2O_3[53,54] etc.are also obtained successfully. No other oxide has been given as much interest as SiO_2 so far. The available literature mostly covers SiO_2 systems to understand the coating phenomena and subsequent oxide formation. Presently the research is getting diverted towards other oxides also like ZrO_2 after recognising the potential use of these coatings. The following section gives the brief review of the work done in obtaining ZrO_2 coatings so far by the sol-gel process.

I.2.b **Literature Survey**

Sim et al[4] applied ZrO_2 coatings by electrophoretic and thermophoretic methods to protect carbon-carbon composites from oxidation. The equivalent oxide concentration of colloidal sol of zirconium hydrate was nearly 3% by weight. Useful

oxidation resistance upto 1000°C was achieved. Large volume changes that result when pure ZrO_2 transforms from the tetragonal to monoclinic form at about 1200°C potentially damage the coating and reduce its effectiveness. Multiple coatings gave improved oxidation resistance (presumably because of over coating pin holes).

ZrO_2-SiO_2 coatings on E-glass fibres to improve their resistance to alkaline attack in cementious composites have been used[39,40]. The presence of ZrO_2 in the coating improves the alkali resistance.

Thin SiO_2-TiO_2-ZrO_2 films from alkoxide solutions were obtained by Beir et al[41]. The effect of formamide ($HCONH_2$) on the gelling time was studied. The chemical durability of the substrates against boiling NaOH solution is enhanced by these coatings. ZrO_2 is considered to be the most important component in this respect. IR spectra of these films are dealt with Nogami et al[55]. Good SiO_2-TiO_2-ZrO_2 glass coatings are obtained when the withdrawal speed in dip coating was 5 cm/min. The oxide system SiO_2-TiO_2-ZrO_2 glass is difficult to study by normal melting techniques. This needs very high temperature, besides, crystallization and/or phase separation would occur. But the sol-gel process makes it simple to get multicomponent oxide systems like this.

Bel Hadj et al[56] have used dip coating route in organometallic solutions to deposit thin films of TiO_2 and ZrO_2 on window glass substrates. The chemical durability, alkali resistance and mechanical strength of the window glass substrates are improved by ZrO_2 coatings. The volume ratio of alkoxide and alcohol was 0.111 for ZrO_2 coating.

The basic sol-gel transition is same for either coatings or monoliths. It is worth while to consider the work that has been done related to ZrO_2 monoliths. Sol-gel transition in zirconia systems using physical and chemical processes have been studied by Guizard et al[57]. Two routes are described to achieve the formation of stable sols and the conversion of sols to gels in multicomponent systems with zirconia as a major component. The first class of gels are obtained from submicron sized particles which lead to high reactivity and lower processing temperatures owing to their high specific surface energy. Such gels are formed in an aqueous medium from colloidal sols where gelation is mainly an electrolytic effect. The second one is a different class of gels in which ZrO_2 oxide network is formed through chemical polymerization in an alcohol medium. Zirconium propoxide is selected as metal organic precursor. As zirconium alkoxides hydrolyse very fast it is necessary to achieve a successful process, to control the hydrolysis reaction in order to avoid precipitation during polycondensation or the formation of unstable colloidal sols. Ethylene glycol forms zirconium glycoxide which hydrolyses slowly. So water addition could be made less critical.

Debsikdar[58] succeeded in obtaining transparent zirconia gel-monoliths from zirconium alkoxide, by controlling the rate of hydrolysis by acetylacetone addition to alcoholic medium. He has observed that zirconium-n propoxide can be stabilized by less than one mole of acetylacetone per mole of the alkoxide. The gel after drying was found to be amorphous to electron diffraction.

The phase transformations that take place during

heating of the amorphous zirconia gel were studied by Debsikdar[59]. Glass like transparent zirconia gel prepared by controlled hydrolysis of zirconium-n-propoxide was subjected to heat treatments ranging from 300 to 800°C. The gel is cleaned and treated with hydrogen peroxide to free it from organics before it is subjected to heating. The gel heated at 400°C contained purely the tetragonal phase. Above 400°C a mixture of tetragonal and monoclinic phases appear. At 800°C only monoclinic phase was observed. The mean average crystallite size after heat treatment in the 400 to 800°C temperature range was of the order of 115°A. The stability of the tetragonal phase of ZrO_2 mainly depends on the nature and amounts of the dopant (e.g. MgO, CaO, Y_2O_3 etc.) But Garvie[60] showed that the kinetics of phase transition of ZrO_2 and phase stability also depends upon the size of the transforming crystals. The monoclinic form becomes unstable with respect to the tetragonal form at 25°C when the grain size is below 30 nm[61]. The presence of anionic impurities[62] can also effect the amorphous to tetragonal transformation. It has been suggested that appearance of the tetragonal phase during heat treatment of the gel at low temperatures might be related to its molecular structural configurations and crystal growth characteristics to the presence of porosity in the gel structure.

In contrast to Debsikdar's method, Kundu et al[63] have prepared monolithic zirconia gels from zirconium-n-propoxide in a nonpolar solvent likl cyclohexane. The nonpolar, hydrophobic solvent was used to avoid precipitation caused by the high rate of hydrolysis of $Zr(OC_3H_7)_4$. They have also obtained amorphous ZrO_2 coatings[64] with isopropanol as solvent. Transparent

coatings can be obtained only upto 2.5 equivalent wt% ZrO_2 in the solution, with isopropanol as solvent. Uncontrolled hydrolysis and precipitation of the hydrated oxide from more concentrated solutions gıve hazy to opaque layers. But with nonpolar solvents like cyclohexane or benzene, transparent coatings can be obtained from concentrated solutions containing 5.5-8 wt% of ZrO_2. The nonpolar benzene or cyclohexane molecules surround the alkoxide polymeric units and act as hydrophobic layers and resist the attack of highly polar H_2O molecules thus suppressing the rate of hydrolysis. Kundu et al[64] could obtain coatings from solutions containing 5.5 wt% of ZrO_2 when the solvent was a non polar cyclohexane.

Zirconium acetylacetone was used to obtaın ZrO_2 films by Pavlov et al[65]. The electron microscope and AES study showed that films prepared at 400°C are amorphous, the short range being the same as in monoclinic ZrO_2. Thermal treatment at 450-800°C leads to crystallization of cubic ZrO_2 which is stabilized with carbon. Heating to 900°C leads to formation of monoclinic phase.

Takahashi et al[66] have used glycol to suppress the rapid hydrolysis and precipitation of zirconıum n-propoxide to get homogeneous ZrO_2 films. A glycol/alkoxide ratio of 2 in the presence of water forms a stable sol that produces a transparent ZrO_2 sol-gel films. The alkoxide concentration, water/alkoxide ratio, and pulling up rate of the substrate control film thickness. They have concentrated to get the crystal form, refractive indices and densities of the films and also on the effects of additives on the system.

Toghe et al[67] have studied the effect of atmospheric humidity on the transmittance of alkoxide derived ZrO_2 coatings. They applied dipping technique to obtain the coatings.

Ezoe et al[68] started with zirconia oxychloride solution to get ZrO_2 films. Hydrolysis of concentrated zirconium oxychloride solution yields transparent gel films upon drying of the sols. They observed that rod shaped ultrafine particles in the films tended to orient m-b axis perpendicular to the film plane. The orientation increased as gelation occurred more slowly and with increasing firing temperature to 1000°C. Firing shrinkage of films was greater in the thickness than in lateral directions.

I.2.c **Scope of Present Work**

In the present work we aimed at obtaining transparent ZrO_2 crystalline films from zirconium-n-propoxide with isopropanol as a solvent. To get coatings from high concentration solutions (equivalent wt% of ZrO_2 = 7.5%) an external reagent diethanolamine is used. It suppresses the hydrolysis and precipitation of oxides from the alkoxides. The compositions are given in the Chapter 3. The porosity and grain growth development in the films with different annealing times at 1250°C are studied using scanning electron micrographs. Characterization of the films for thickness, quality and bandgap energy is done. The phases present in the films after different heat treatments are studied by X-ray diffraction and are compared with those of powders after same heat treatments. Attempts have been made to stabilize ZrO_2 by doping the sol with yttrium nitrate salt, and thus obtained ZrO_2 is analysed for

stabilization by X-ray diffraction technique. The thermal analysis of the unstabilized ZrO_2 powder is done and the results are believed to hold good for the films.

I.3 Fundamentals of Film Formation By Sol-Gel Method

I.3.a Solution Characteristics

The solutions used for coatings should possess some important characteristics as follows:

1) Adequate solubility of the initial compounds is needed. They should have tendency towards crystallization during evaporation of the solvent. These conditions are principally met by those materials which either dissolve in a colloidal or in a polymeric state, or pass over into such a state by reaction with the solvent.

2) Sufficiently small contact angles between the solution and the substrates to be coated give good wetting. The surface structure and the surface cleanliness of the substrate also affect the wettability. In some cases wetabbility can be enhanced by adding wetting reagents to the solutions.

3) Adequate durability of the solution and constancy of processing conditions. Often stabilizers are used to make processing feasible under steady conditions.

4) Transformability of the deposited gel film into a solid homogeneous oxide layer. By drying and heating of the films, high bonding strength to the substrate should be formed. On solidification the film should not crack or haze. Therefore, film components which are released during the solidification should not have an excessive volume content in the gel layer.

I.3.b Coating Techniques

The liquid coatings can be obtained by using any one of the following processes:

1) Dipping Process

Substrates to be coated are withdrawn from the solution and get covered with a liquid film.

2) Lowering Processes, in which the object remains at rest and the liquid level is lowered. The required layer thickness can be kept under control by measuring the rate of flow with a flow meter.

3) Spinning Processes

It is done by spreading out the liquid film by spinning wetted surfaces, it is suitable for small circular disks or lenses only. There are no marginal disturbances. The solution poured on a rotating approximately horizontal substrate, spreads out on its surface completely and evenly. The thickness can be controlled by controlling the rotational speed. This process is less economical than others.

4) Spraying Process

These are suitable for nonoptical coatings since it is very difficult to obtain homogeneous films of sufficiently uniform thickness with this technique. The solution to be sprayed is squirted out of one or several stationary spray guns onto the preheated glass plate which is moved across the jets at a predetermined speed.

I.3.c Dip Coating

It is most economic method for obtaining coatings on large surfaces on both sides. The substrate to be coated is

lowered slowly into the solution containing hydrolysable metal compounds in a container. The lifting movement of the carrier from which the substrates to be coated are suspended, must be completely smooth and shockless. The substrates should be withdrawn from the solution slowly. The film formation on the substrates develops very uniformly along the horizontal dipping line, provided that the operation is not disturbed by irregularities in the liquid level by uncontrolled air currents. When the lifting speed is sufficiently slow, the thickness distribution in the vertical direction will be defined only by the evaporation of the solvent. So in order to get constant thickness of the solid film along the lifting direction it is necessary that the pulling rate be small. A pulling rate of 5 cm/min gives generally good homogeneous films.

When the substrate is withdrawn from the solution the liquid film partly flows down the substrate and partly adheres to it. This solidifies after the evaporation of the solvent, as both hydrolysis and condensation reactions take place. After drying this liquid film one gets a gel film. Finally, the film is hardened in a high temperature cycle until a transparent metal oxide film has been formed. Detailed study of the reactions is dealt in the next section.

The thickness 't' of the solid layer finally obtained depends mainly on the following parameters:

1) Speed (V) of the lifting movement
2) Angle of inclination (θ) of the coated surface relative to the horizontal line
3) Concentration (C) of the solution
4) Viscosity of solution

5) Surface tension

6) Vapour pressure of the solution

7) Temperature

8) Atmospheric humidity

For a given solution (parameters 4,5,6 are fixed) if the temperature and humidity are kept constant the thickness of the coating is determined only by V and θ. The dependence on V can be expressed as $t \propto V^{2/3}$. The log (thickness) Vs. log (V) graphs show a slope of 1/2 to 2/3[50] for alkoxide solutions. This implies simultaneous effect of gravity as well as viscosity and surface tension of the solution on the formation of the coatings. With the increase of concentration the viscosity of the solution increases. So there is a nonlinear relation between 't' and the concentration (C) of the solution.

When substrates are immersed in the solution care has to be taken not to dip the clamps or other holding devices. Otherwise the solution residues pass onto the surface that is to be coated and so spoil the appearance. The lower edge of the substrate will always have certain width of higher thickness zone, caused by the adhering liquid residues. The width of this trouble zone can not be fully eliminated. However it can be minimised by reducing the viscosity of the solution. The width of the trouble zone also depends on the shape of the edge and the lifting speed. Its width generally extends from 2-8 mm. For more viscous solutions it is even more than this. For large substrates it is advisable to cut off this edge rather than to vary the conditions to have minimum width.

Thicker coatings can be obtained either by increasing the pulling speed or by multiple dipping. Multiple dipping

gives thicker films than the other method. After each dip the coating is to be dried before it is reimmersed into the solution.

Since, in thin coatings, both the in-diffusion of the water required for hydrolysis and the out diffusion of the condensation products proceed well controlled, such coatings on large - area surfaces are extremely uniform, homogeneous and dense[36].

The dip coating technique offers the following advantages:

1) Highly homogeneous layers of almost any thickness can be produced.

2) Many different metal oxide layers can be coated onto one another.

3) Very large surfaces (12 m^2) can be coated[36].

4) The cost of dip coating method decreases in many cases with increasing dimensions of the object. But investment cost is high.

5) Economical and also gives good coatings with good mechanical and chemical stability. It competes with vacuum coating methods, spraying processes and chemical vapour deposition processes.

6) Dip coating method is much more empirically established than its competing processes.

7) Both sides of a substrate can be coated simultaneously whereas in vacuum coating it is very difficult.

8) Inside and outsides of tubes of various diameters and shapes can be coated successfully. But with vacuum evaporating technique it is very difficult.

9) Large plates can be coated easily with dip coating processes. Vacuum techniques need considerable effort.

I.3.d **Chemistry**

In the sol-gel process generally the solution is prepared from the alkoxides of the metals. The metal alkoxides are hydrolysable. The products of the hydrolysis are metal hydroxides in a gel form. When the gel is heated to high temperatures the entrapped solvents and water etc. are removed and an amorphous metal oxide forms. The alkoxides can absorb the moisture from the atmosphere and undergo hydrolysis. But for coatings the solutions should have some life period before the precipitation of oxides take place. This demands the stabilization of the solutions. The zirconium alkoxide is very much active as compared to silicon alkoxide. The reactivity of the alkoxide vary from one to another. A less reactive alkoxide is easier to handle for coating. To get transparent metal oxide layers, hydrolysis and condensation have to take place slowly and more or less simultaneously, thus initiating the formation of a gel like structure.

The main reactions are as shown below:

$$Zr(OR)_4 + 4H_2O \rightarrow Zr(OH)_4 + 4\ ROH$$

$$Zr(OH)_4 \xrightarrow{\text{(heat)}} ZrO_2 + 2H_2O \qquad (1)$$

These are simplified reactions. The actual reactions are much more complex and take place in steps. On hydrolysis,

zirconium alkoxides form hydrous zirconium oxide, $ZrO_2\ nH_2O$ or $ZrO(OH)_2\ n\ H_2O$ and/or zirconium oxide alkoxides, which are hydrated polymeric species having a number of Zr-O-Zr bridges. Zirconium oxide alkoxides are condensation-coordination polymers based on octahedrally 6-coordinated zirconium[58]. Hydrolytic polycondensation reactions of zirconium alkoxides result in the formation of Zr-O-Zr bridges according to

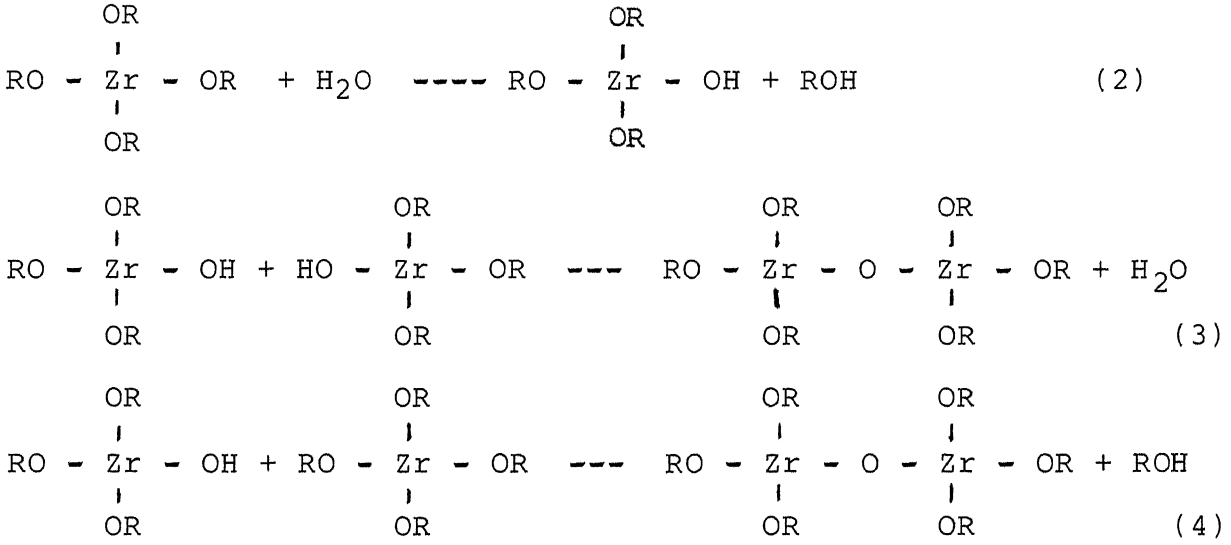

where R = C_2H_5, C_3H_7 or C_4H_9 etc. In addition, there may be coordination polymerization involving either the alkoxide oxygen or the oxo-oxygen or both. If not controlled, the reaction (2) is much faster than reaction (3) and (4) and results in precipitation. However controlled hydrolysis will give soluble polymeric intermediates(or sol) which undergo further polymerization to form a clear gel.

The alkoxide and water are immisible. To carry out the reaction between these two a common solvent is needed. Generally, alcoholic medium is used. The mixture of alkoxide and alcohol solutions are added to the mixture containing

alcohol and the required amount of water. If the alkoxide is active like zirconium-n-propoxide, then the presence of an external reagent is needed to suppress the hydrolysis and precipitation of the oxides. Ethelene glycol, diethelenеglycol, diethanolamine etc. are generally used[46] for this purpose. In the presence of these, the water content in the solution will have less effect on the transparency of the final layers. Otherwise, the water content is very critical. If it is less then discontinuous films form and if it is more then rapid gel formation will take place[46]. Since glasses and ceramics always; and metals frequently due to their oxide layers, carry surface OH groups, the bonding is ideal. The oxide structure of the glass is extended into the layer. Dip coating method involves many more chemical reactions than any other coating method. At temperatures around 100°C the films still contain many OH groups and therefore are hydrophilic and soft. On heating them above 300-400°C they become hard and strong. These will be amorphous in nature. To get crystalline coatings one has to go for still higher temperatures. Film forming oxides are mainly those of the elements of the group III-VIII of the periodic table, e.g. Al, In,Si, Ti, Zr,Sn, Pb, Ta, Cr,Fe, Ni, Co.

Figure I.1 schematically shows the dip coating process. The film formation differs from bulk gel or 'monolith' in certain respects[69] as shown below:

1) Films are normally deposited from dilute solutions in which individual solution species are initially weakly interacting or non interacting. During deposition the rapid increase in concentration (18-36 fold) resulting from

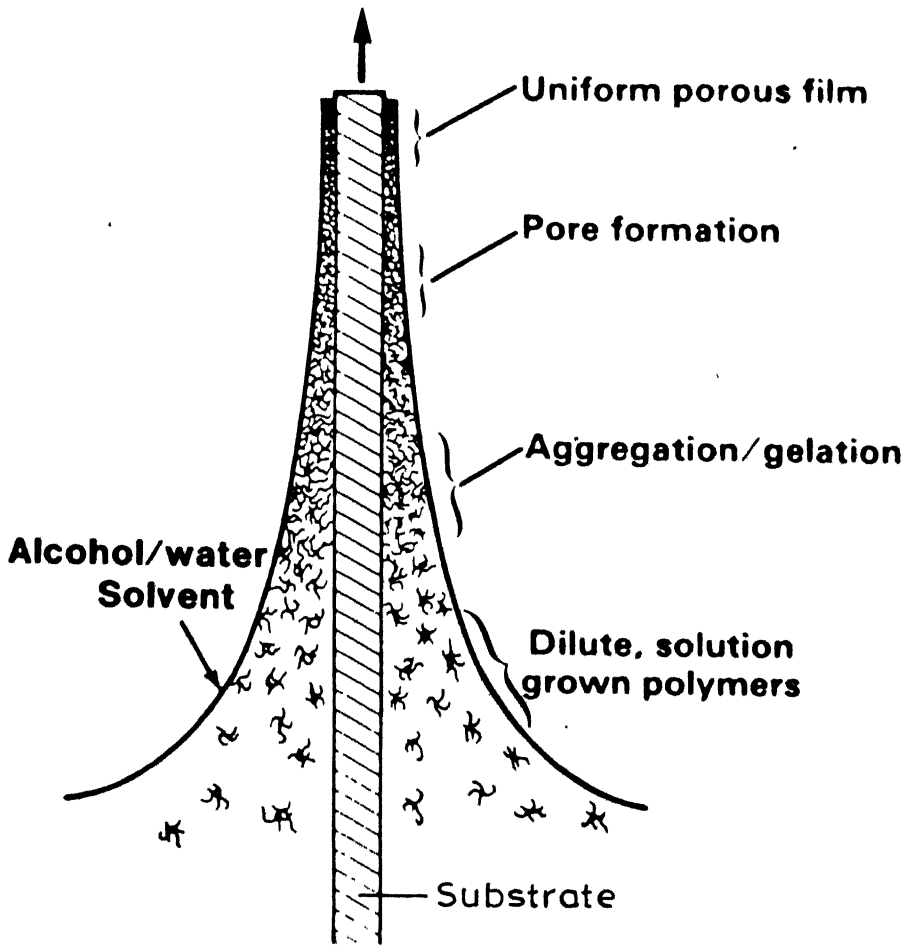

Fig. I.1 Schematic representation of the dip coating process.(69)

evaporation, forces the precursors into close proximity with each other, increasing the reaction rate significantly. Thus a gel coating is formed. Further evaporation of the solvent results in porosity within the film. In contrast to this in the bulk systems the concentrations remain constant during gelation and increase only during drying.

2) Concentration - induced gelation imposes a time scale for the sequential stage of film formation which depends on the evaporation rate of the solvent. The evaporation compacts the structure while the condensation reactions stiffen the structure. These two compete with each other and finally the resistance to compaction will be increased. Compared to bulk systems, aggregation, gelation and drying occur more rapidly.

3) Fluid flow due to gravity, evaporation or angular acceleration, combined with attachment of the precursor species to the substrate, imposes a shear stress within the film during deposition. After gelation shrinkage, due to removal of solvent and continued condensation creates a tensile stress within the film, while stresses are not present in bulk gels.

I.4 General Features of Coatings

I.4.a Wetting

The wetting behaviour of sol is an important factor in determining the quality of coatings. The wetting behaviour is a complicated function of sol-substrate chemistry. The coating quality can be considerably altered by the choice of substrate,

sol additives and sol ageing etc. Cracking of the coatings is to be avoided since,by cracking the visual appearance as well as protection of the substrate from chemical attack is lost. Fig. I.2 shows three different types of wetting on silica substrates for different compositions of sols[70].

Type 1 - The sol initially wets a small area of the substrate then withdraws to a single bead, and finally remains there until gelation after several minutes.

Type 2 - It is characterized by initial wetting and the withdrawl similar to Type 1. The difference being the withdrawl from both the circumference of the coating as well as from the isolated regions of the previously wetted region.

Type 3 - It is characterized by uniform rapid and extensive spreading of the sol over the substrate. It is necessary to have this type of wetting to get good coating.

Generally soda lime silicate glass substrates are better than fused silica substrate to give good coatings for the same composition of the sol[70]. Neverthless, small but distinct beads of sol material form irrespective of the substrate and the sol composition. But one can reduce the height of these beads by changing the substrate and/or sol composition.

Type 1 - wetting is influenced by unhydrolysed alkoxides in the sol i.e. it is related to the presence of OR groups on alkoxide. Water content in the sol has some effect in wetting. In the absence of high acid concentrations,high water content sols give Type II wetting and low water content sols typically give Type III wetting. To get good coatings one has to go for

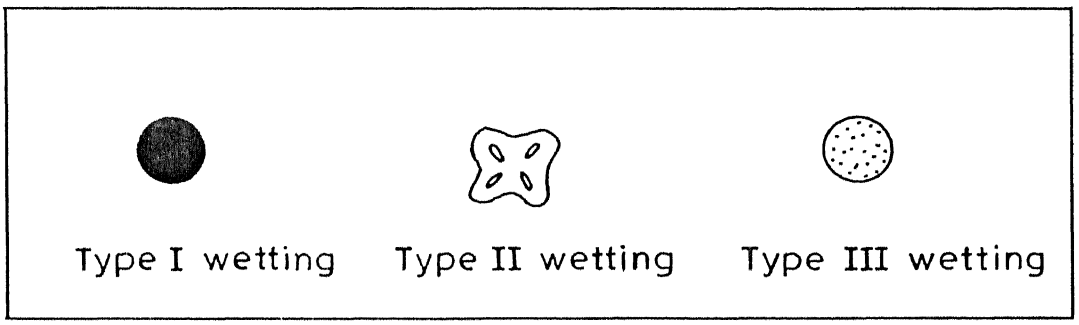

Fig. I.2 Illustration of a single drop of solution on glass substrate exhibiting type I, II and III wetting.

medium water contents.

Additives like Titanium alkoxides etc. to the silicon alkoxide sols improve the quality of the coatings.

I.4.b **Factors Affecting The Thickness**

The factors affecting the thickness of the coatings were briefly mentioned in the previous 'Dip coatings' section. The more detailed discussion is given below.

Landau and Levich[71] dealt with the idealized case of an infinite plate being withdrawn vertically from a vessel sufficiently large aenough to allow boundary effects to be ignored. The properties of the solutions that may affect the thickness of the layer (such as viscosity, density and surface tension) in metal-organic solutions have been experimentally expressed as one parameter[31]. However, some theoretical hydrodynamic models have been proposed in polymer processing for viscous, capillary and high Reynolds number withdrawl[72]. Most of the theoretical and experimental research on capillary withdrawl ($C_a << 1$ and $Re << 1$) shows a dependence of the coating phenomena on the capillary number,

$$C_a = \eta V / \sigma \qquad (1)$$

η = viscosity of the solution

V = withdrawl speed

σ = surface tension

g = acceleration due to gravity

The liquid film thickness 't' is given by[45]

$$t = 0.944 \, (C_a)^{1/6} \, (\eta V / \rho g)^{1/2} \qquad (2)$$

Yang et al[73] investigated the dependence of the coating thickness on the liquid viscosity and withdrawl speed from a solution of 80 mol% styrene and 20 mol% hexylmethacrylate copolymer in toluene. In this case, the following expression was derived for the dried film thickness 't_p'

$$t_p = (J/\xi_p)\{(\eta - \eta_s)/\eta_o\}^{1/\alpha} (\eta V/\rho g)^{1/2} \quad (3)$$

η, η_s are viscosities of the solution and solvent respectively,

η_o and α are the intercept and gradient of a plot of log $(\eta - \eta_s)$ vs. log C_p

C_p is the mass concentration of the polymer solution

ξ_p is the ratio of the densities of the polymer and to the solution, and

J is a dimensionless flow parameter given by $j/V\ t_o$, where j is the volume flow rate per unit width and t_o is a characteristic thickness, given by

$$t_o = (\eta V/\rho g)^{1/2} \quad (4)$$

In deriving eq. (3) a low capillary number C_a was assumed by Yang et al.

I.4.c Factors Affecting the Quality of Coatings

In metal alkoxide systems other than silicon, the hydrolysis reactions often lead to precipitation of insoluble condensates, thus making the solution unsuitable for optical

coating applications. Schroeder(74) has allowed the atmospheric humidity to hydrolyze the alkoxides on the substrate after it was applied. In recent years the technology is developed to prepare clear polymerized solutions in almost any oxide system without the aid of humid atmosphere. The preparation of these solutions by varying the hydrolysis and polymerization reactions introduces structural and morphological modifications into the inorganic network of the polymer species in the solution. Thus the properties of the inorganic films deposited from these solutions may show differences without compositional variations due to:

1) Molecular structural variations in the polymer network of the precursor species.

2) Morphological factors introduced by the deposition method, i.e. spin or dip coating.

The main parameters that modify the structure and properties of the alkoxide-derived solutions deposited films may be listed[75] as follows:

1) Selection of starting compound and the solvent
2) Water/alkoxide ratio
3) Molecular separation by dilution
4) Catalytic effects
5) Temperature and length of reaction time
6) Deposition methods.

Spin coating results in a film morphology which is more porous and more resistant to sintering than dip coating (from the same solution). Dip coating yields smoother coatings than spin coating method.

Higher water in hydrolysis of alkoxide solutions results

in denser film morphologies.This may or may not be true for other systems.

A high water (low concentration) solution deposits a smoother coating than one of low water (high concentration). The alcohol used also affects the quality of coating. For silicon alkoxide systems ethanol is preferred to propanol.

I.4.d **Applications of Sol-gel Derived Coatings**

Applications of sol-gel derived coatings are many in number. The Table I.1 gives certain areas of application. However it is not exhaustive. The applications of ZrO_2 coatings are discussed previously. So the Table I.1 is essentially made in view of other materials. More detailed list of applications of the sol-gel derived coatings can be obtained from Ref.77,78.

I.4.e **Phase Transformations in Sol-gel Derived Products**

X-ray investigations of ZrO_2 powder produced under different hydrolysis conditions show significant differences in the ZrO_2 structure as a function of hydrolysis water. The alkoxide structure initially favours the formation of the amorphous or cubic phase, which later transforms to the monoclinic phase by thermal activation at 600-1000^oC[79]. Table I.2 gives the relative phases present.

Applications of Dip Coated Films Prepared By Sol-gel Method[76]

Purpose	Example	Composition	Authors
1. Mechanical protection	Protection of glass or metal	SiO_2	Yamamoto et al
2. Chemical protection	Increase of durability passivation of Si	GeO_2-SiO_2	Schlichting and Newman
3. Optical properties	Coloured film	TiO_2-SiO_2	Dislich and Hinz
		SiO_2-transition metal oxides,	Yamamoto et al
		Oxides of Fe,Cr and Co	Geotti-Bianchini et al
	Reflecting film	In_2O_3-SnO_2	Arfsten
	Antireflection film	Na_2O-B_2O_3-SiO_2	Mukherjee and Lowdermilk
4. Ferroelectricity	Capacitor	$BaTiO_3$	Sakka,Sakka Kokubo,Yanovskaya et al
		$BaTiO_3$,$KTaO_3$	Wu et al
5. Electrical conductivity	Electronic conductive film	In_2O_3-SnO_2, SnO_2-CdO	Ogiwara and Kinugawa
		CdO	Dislich and Hinz
	Ionic conductive film	β-alumina	Yoldas and Partlow
6. Catalyst	Photocatalyst film	TiO_2	Yoko et al
	Catalyst carrier	SiO_2,TiO_2, Al_2O_3	

Table I.2

Effect of Hydrolysis on the Amount of Monoclinic Phase of ZrO_2

Hydrolysis water (mole/mole alkoxide)	% Monoclinic phase transformed after 30 minutes at		
	600°C	800°C	1000°C
1	14	24	87
10	39	77	86

CHAPTER II

EXPERIMENTAL PROCEDURES

II.1 Sample Preparation

II.1.1 Chemicals and Substrates

The chemicals and substrates used for the preparation of zirconia coatings and powders are as follows:

a) Zirconium-n-propoxide supplied by Alfa Morton Thikol, Inc., USA.

b) Iso propanol supplied by S.D. Fine Chem. Pvt. Ltd. Boisar AR grade. The chemical analysis is given in Table II.1

c) Diethanolamine (DEA) supplied by BDH with a minimum assay as 99%. It was further distilled in the laboratory to get it more purified.

d) Triple distilled water made in the laboratory, in a quartz distiller.

e) Sapphire (α-Al_2O_3 $(11\bar{2}0)$ orientation) single crystals, microscope glass slides are used as substrates for coatings.

II.1.2 Preparation of Zirconia Coatings and Powders

The zirconia coatings are obtained on substrates by dip coating method from the sol made up of zirconium-n-propoxide (ZrnP), H_2O, DEA and isopropyl alcohol. The chemical reactions that occur are given under the section 'Chemistry' (I.3.d) in

Table II.1

Chemical Analysis of the Isopropyl Alcohol Supplied by S.D.Fine Chem. Pvt. Ltd. Boisar (Manufacturer's Data)

	Percent by wt.
Thermal assay	99.5%
H_2O content	0.1%
Acidity (C_2H_5COOH)	0.01 ml.N/1%
Alkalinity	0.01 ml.N/1%
Non-volatile mattre	0.002%
Aldehydes and ketones	0.005%
Impurities determined by GLC	0.2%

the Chapter I.

The powders of the stabilized and unstabilized ZrO_2 are obtained by allowing the respective sols to become gels by leaving them to absorb moisture. The subsequent drying of the gels give rise to powders.

II.1.3 Substrate Preparation for the Coating

The substrates (sapphire single crystal $(11\bar{2}0)$) are first cleaned with fresh water to remove the dust particles from the surfaces. After drying,they were polished on 4-0 emery paper to remove any previous coatings. This also helps in polishing away any deep rooted scratches that were present. The substrates are then cleaned with running water and soap. The dimensions of the substrate were 13 mmx 11 mm x 1 mm. The microscopic glasses (the new ones) and the above cleaned sapphire substrates are given the final cleaning treatment as given below before giving them a coating.

1) Soaking the substrates in dilute HCl for 5 min
2) Wash with water and detergent
3) Ultrasonication in acetone bath for 5-10 min
4) Rinse with ethyl alcohol
5) Dry in the oven (temperature $50^{o}C$) for 15 min

During the cleaning procedure the substrates are handled with forceps to prevent the formation of finger prints on the substrates. The substrates are hung in the oven with the help of crocodile clips so that they do not touch the walls of the oven during drying. Clean substrates are stored in a covered petridish and kept in a dust free chamber.

II.1.4 Sol-Preparation

II.1.4.a Unstabilized ZrO_2 Coatings and Powders

For all the coatings and powders of unstabilized ZrO_2, a constant composition which is given in Table II.2 is used. This composition is selected after trying with a number of other compositions to get transparent and sufficiently thick coatings.

Decrease of ZrnP content resulted in very thin coatings and decrease of DEA in powdery coatings. The molar ratio of DEA/ZrnP = 0.74 is found to be giving reasonably good coatings.

To make a 20 ml of the sol the required amounts of the constituents are calculated as shown below.

1) Zirconium-n-Propoxide (ZrnP)

Molecular weight	=	327.57
Density	=	1.05 gm/cm^3
Volume of 1 mole of ZrnP	=	$\frac{327.57}{1.05}$
	=	311.95 cm^3
To make 1000 ml of sol, (0.5 M concentration of ZrnP) ZrnP needed	=	155.98 ml
To make 20 ml of sol, ZrnP needed	=	3.1 ml

2) Diethanolamine (DEA)

Molecular weight	=	105.14
Density	=	1.098 gm/cm^3
Volume of 0.37 mole of DEA	=	0.37x95.76
	=	35.90 ml
To make 1000 ml of sol DEA needed	=	35.9 ml

Table II.2

Composition of the Sol Used for Unstabilized ZrO_2 Coatings and Powders

Constituents	Concentration	
	Mole lit^{-1}	ml in 20 ml
1. Zirconium-n-Propoxide (ZrnP)	0.5 M	3.1 ml
2. Diethanolamine ($\frac{DEA}{ZrnP}$ molar ratio = 0.74)	0.37 M	0.71 ml
3. Distilled water ($\frac{H_2O}{ZrnP}$ = 1.8)	0.9 M	0.324 ml
4. Isopropyl alcohol	Solvent	15.87 ml

To make 20 ml of sol DEA needed = 0.71 ml

3) Water (H_2O)

Molecular weight = 18

Density = 1 gm/cm^3

Volume of 0.9 mole H_2O = 0.9x18

= 16.2 ml

To make 20 ml of sol water needed = 0.324 ml

4) Isopropyl alcohol

It is the common solvent used, so amount needed

= (Volume of the sol – Volume of (DEA+ZrnP+H_2O))

= 20-(0.71+3.1+0.324)

= 15.87 ml

Equivalent Weight% of ZrO_2 In Solution

Weight of ZrnP in 20 ml of sol = 3.1x1.05 = 3.255 gm

Weight of DEA in 20 ml of sol = 0.71x1.098 = 0.77958 gm

Weight of H_2O in 20 ml of sol = 0.324x1 = 0.324 gm

Weight of isopropyl alcohol in 20 ml of sol

= 15.87x0.785 = 12.454

Total weight of 20 ml of sol = 16.8134 gm

Molecular weight of ZrO_2 = 123.22

ZrnP —— ZrO_2

327.5gm —— 123.22 gm

3.255gm —— 1.2247 gm

Weight % of ZrO_2 in sol is = $\frac{1.2247}{16.8134} \times 100 = 7.3\%$

The apparatus used during sol preparation viz. pippettes, beakers, teflon covered magnets for magnetic stirring, measuring cylinder etc. are thoroughly cleaned before use with chromic acid then with a detergent and finally with triple distilled water.

A quick rinse with acetone is given after washing and this helps in fast drying. The apparatus are dried well, in the oven kept at 50°C.

Initially, 15.87 ml of isopropyl alcohol is taken into a measuring cylinder. Then 0.71 ml of DEA is measured with a pippette and transferred into a dried beaker. Immediately nearly half of the measured quantity of isopropyl alcohol from the measuring cylinder is poured into the beaker containing the 0.71 ml of DEA. The pippette used is rinsed with some more propanol from the measuring cylinder and the washing is also mixed with the contents in the beaker.

3.1 ml of ZrnP is measured with another pippette and is transferred into the beaker containing DEA and isopropyl alcohol mixture. The rinsing of the pippette is done with some alcohol from the measuring cylinder and these washings are also mixed with the contents in the beaker.

The teflon covered magnet is slipped into the solution and the top of the beaker is covered with an aluminium foil to prevent the moisture absorbtion from the atmosphere. To prevent any air leakage the foil is kept tight with the help of a cellophane tape. The solution in the beaker is stirred for 2 hrs using a magnetic stirrer till a transparent clear solution is obtained.

The remaining alcohol in the measuring cylinder is mixed with 0.324 ml of triple distilled water. This solution is added to the initial solution after 2 hrs of its stirring. The mixture of these two solutions is allowed to stir for 15 more minutes. A clear transparent sol is obtained at the end of this stirring and mixing cycle. The sol is allowed to stand for some time before it is used for coating.

II.1.4.b **Stabilized ZrO_2 Powders**

The high temperature tetragonal/cubic phase can be stabilized by doping ZrO_2 with Y_2O_3. In the present case during the preparation of ZrO_2 through the sol-gel method, Y_2O_3 is incorporated in the ZrO_2 lattice by the addition of yttrium nitrate salt to the sol. The addition is easy because the yttrium nitrate is soluble in isopropyl alcohol which is also used as a common solvent for the alkoxide and the water.

The standard compositions as shown in Table II.3 are used for obtaining the stabilized ZrO_2 powders. There is no need for the addition of water externally, as the salt itself has 6 molecules of water in it per mole.

The 0.6615 gm of yttrium nitrate per 20 ml of sol would give rise to an amount of yttrium oxide which is about 8 mole % in the final ZrO_2 powder. The calculations are as follows:

Yttrium nitrate formula weight	$Y(NO_3)_3.6H_2O$	= 383.01
Yttrium oxide formula weight		= 225.81
ZrnP formula weight		= 327.56
ZrO_2 formula weight		= 123.22

Table II.3

Composition of the sol used for stabilized ZrO_2 powders.

Constituents	Amounts
Zrnp (conc. 0.5M)	3.10 ml
D E A (DEA/Zmp molar ratio=0.71)	0.71 ml
Yttrium Nitrate	0.6615 gm
Isopropanol	16.0 ml

The concentration of ZrnP in the solution = 0.5 mole/lit

ZrnP gives ------ ZrO_2

0.5 mole of ZrnP gives ---- 0.5 mole of ZrO_2

Required concentration of Y_2O_3 in ZrO_2 = 8 mole%

In the present case moles of Y_2O_3 needed = 8/92x0.5

= 0.0434

2 $Y(NO_3)_3.6H_2O$ -------- Y_2O_3

1 mole of Y_2O_3 comes from --- 2 moles of yttrium nitrate salt.

0.0434 moles of Y_2O_3 comes from ----- 0.0841 moles of yttrium nitrate

The amount to be added per litre of solution

= 0.084 moles of yttrium nitrate

The amount to be added per 20 ml of solution

= 0.0017 moles

1 mole of yttrium nitrate weighs = 383.01 gm

0.0017 moles of yttrium nitrate weighs = 0.66 gm

The water content present in 0.66 gms of the salt is calculated to be 0.186 ml.

The sol preparation is exactly similar to what is explained previously under the section II.1.4.a "Sol Preparation for Unstabilized ZrO_2 Coatings and Powders" except for the addition of salt to propanol instead of water. The ZrnP, DEA and propanol mixture is kept for stirring for 2 hrs. The weighed amount of yttrium nitrate 0.66 gm is dissolved well in the remaining propanol. At the end of stirring both the solutions are mixed and an immediate gelling is resulted. The gel is allowed to dry in the air for 2-3 days and then kept in the oven at 50°C for further drying.

The attempts made to dope the ZrO_2 coatings with Y_2O_3 have failed. The immediate gelling after the addition of yttrium nitrate and propanol solution to the solution of ZrnP, DEA and alcohol, is to be prevented to get stabilized coatings. Attempts were made to prevent gelling by adjusting the pH. The addition of ammonia to the salt propanol solution to increase the pH resulted in precipitation of yttrium ions as yttrium hydroxide. The addition of sodium hydroxide was also found to be ineffective. The change of salt to yttrium chloride has not worked as it is not dissolvable in propanol, easily.

II.1.5.a **Coating Technique**

The substrates are coated by dip coating technique. Thickness of the coatings is increased by multiple dipping with intermediate drying in the oven kept at 50°C. The substrates are carefully inserted into the sol and then pulled out at a constant speed into the room atmosphere.

An A.C. synchronous reversible motor (240 V, 1 phase, 50 Hz, 120 mA Vishal.Syn.No. 7129) is used to drive a pulley of very large diameter. The diameter ratio of the motor gear and the pulley is approximately 15. A rod of dia 4 mm and length 10 cm is positioned tightly at the centre of the pulley. This rod is adjusted to make it horizontal. A long cotton thread with one end tied to 'O' ring is hung from this rod. As the pulley rotates the thread winds onto the rod and the samples hung from the 'O' ring can be moved up or down. The setup is shown in Fig. II.1 schematically. The pulling or dipping can be done by changing the direction of rotation of the pulley. The pulling speed is found to be approximately 5 cm/min by measuring the

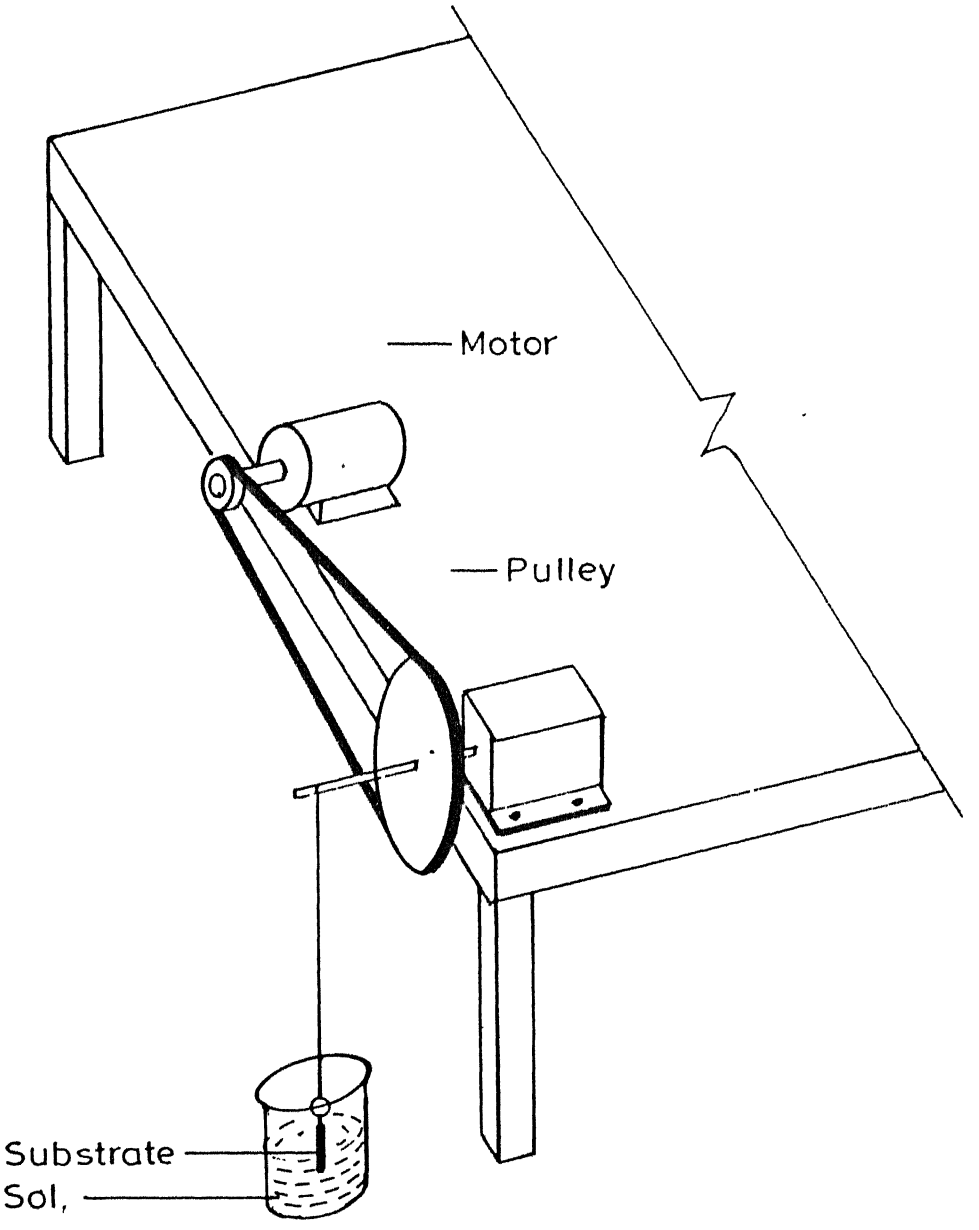

Fig. II.1 Setup for dip coating.

distance moved by a marked point on the thread in a specified time.

The substrate is hung from the 'O' ring at the end of the cotton thread with the help of a crocodile clip. The beaker containing the sol is placed directly beneath the substrate at some distance. The substrate is slowly lowered by running the motor and allowed to dip without touching the walls of the beaker. Care is taken to prevent the vibrations of the thread from the air currents. After dipping to required depth the substrate is slowly withdrawn by changing the directon of rotation. The liquid layer forms a coating on the substrate and this is allowed to dry for 10 min in the dust free open air atmosphere. After this, the coated substrate is transferred to a oven kept at 50^{o}C and is allowed to dry. The above cycle of dipping - air dry - oven dry is repeated for a number of times to get thicker coatings. Four different thicknesses are obtained by coating the substrate once (Sample 1) twice (Sample 2) thrice (Sample 3) and four times (Sample 4).

II.1.5.b **Gel (Powder) Preparation**

The sol left after the coating has a shelf life of 7-9 days and after this it forms a gel. This gel is dried by keeping it in a oven at 50^{o}C. The dried gel is crushed into powder and is used for phase analysis after different heat treatments.

II.1.6 **Heat Treatments**

II.1.6.a Some of the oven dried unstabilized ZrO_2 coatings (four different thicknesses) are heated to 600^{o}C at a slow

heating rate of approximately 2°C/min from the room temperature in a furnace. These are kept at 600°C for 2-3 min. and are cooled down to room temperature at the same rate. The coatings thus treated were used for the thickness and band gap energy measurements.

II.1.6.b The other oven dried unstabilized ZrO_2 coatings on sapphire are given heat treatments at 1250°C for different lengths of time to study porosity and grain growth developments.

Four different coating thickness samples (viz. Sample 1, Sample 2, Sample 3 and Sample 4) are taken, and each one of them is broken into four small pieces by cleaving them along the cleavage plane. In this way four sets of samples containing four different thicknesses in each set are made. Each set is kept for a different length of annealing time at 1250°C as shown below:

Set 1 - 5 min

Set 2 - 30 min

Set 3 - 4 hrs

Set 4 - 8 hrs

Heat treatments are given in an air atmosphere in an horizontal tube furnace. The samples are slowly introduced into the furnace, to minimize the thermal shock. The withdrawl of the sample from the furnace is also done slowly, after keeping for the stipulated time at 1250°C. The coatings are covered by another crucible to prevent any dust accumulation or impurity deposition from the furnace, during the heat treatments.

II.1.6.c The unstabilized ZrO_2 powders and coatings are given different heat treatments to study the sequence of phase

changes. The coatings did not change the colour with the temperatures, but they became less transparent with rise of temperatures of the treatments. It is believed to be due to porosity development and/or increased grain boundary scattering. The powders had different colours after different heat treatments as shown below:

Temperature	Time	Colour of the Powder
260°C	2.5 hrs	Yellowish black
325°C	2.5 hrs	Black
450°C	2.5 hrs	Whitish black
625°C	2.5 hrs	White
905°C	2.5 hrs	White
1250°	2.5 hrs	White

II.1.6.d The stabilized ZrO_2 powders obtained after drying the gel in the oven are treated at 1250°C for 2.5, 3.5, 5 hrs to make three samples for the phase analysis.

II.2 Characterization of the Coatings

II.2.1 Optical Microscopy of the Coatings

The coatings are examined using an optical microscope (Zeiss West Germany) under reflected light at a magnification of 100X after drying in air at 50°C for 15 hrs and after further baking at 600°C for 2-3 min.

II.2.2 Thickness Measurements

The thicknesses of the baked coatings are determined using two techniques:

A) Profilometry

B) Double beam interferometry.

II.2.2.a **Profilometry**

An Alpha step 200 (Tencor Instruments, USA) is used to measure the thickness. The instrument scans a diamond stylus over the sample and directly measures the step height between the substrate and the film. The heat treated film cracks at many places and provides natural steps for such measurements.

II.2.2.b **Double Beam Interferometry**

Mirau double beam interference equipment in combination with Zeiss Universal Microscope is used for the determination of thickness of ZrO_2 coatings on transparent sapphire single crystal substrate. The measurement is contact free so that specimen surface and interference optical parts are not damaged. The interferometer is supplied by Carl Zeiss Company, West Germany.

The Fig. II.2 shows the schematic diagram of the setup and the path of the monochromatic light during the measurement. The interference figure is produced by the interaction of two coherent beams which originate from splitting of the light leaving the objective (2.2) by the interference beam splitter (2.5). After reflection by the coating (2.6)and the mirror (2.3) of the reference plate (2.4) the beams combine and interfere and produce interference fringes. The fringes become sharper and background intensity falls to a smaller value as the reflection coefficient increases[80]. Irregularities of the specimen surface change the path difference of the optical paths

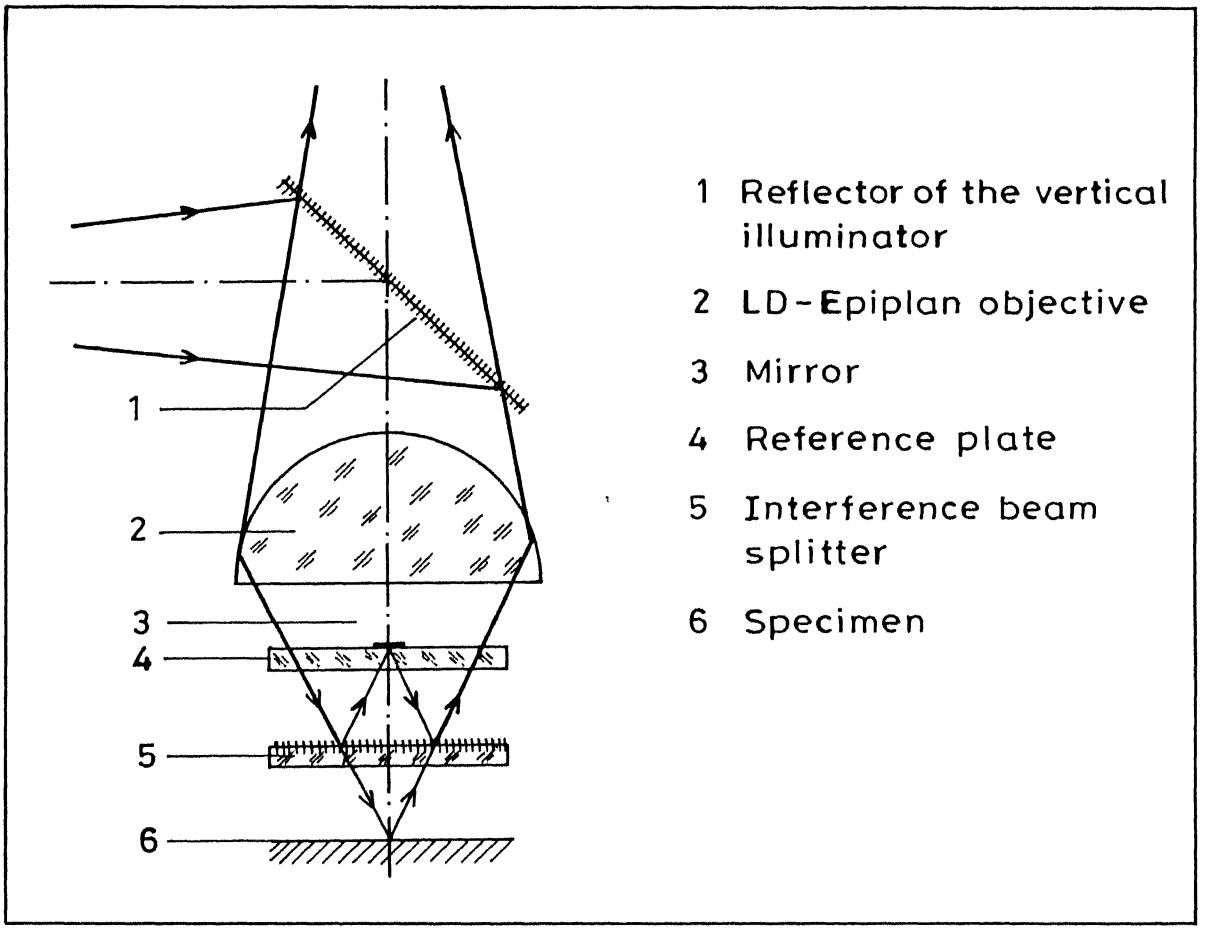

Fig. II.2 Interference equipment setup and the path of rays.

covered by the beams, and cause deflection of the fringes.

According to the Airy's formula(80)

$$\frac{I_{max}}{I_{min}} = \left[\frac{1 + R}{1 - R}\right]^2 \qquad (1)$$

I_{max} = Intensity of the fringe maximum

I_{min} = Intensity of the fringe minimum

R = Coefficient of reflectance.

From the above formula it is clear that the whole fringe shape is quite independent of absorption.

The reference plate (2.4) is provided with three mirrors of different reflectivities. The contrast of the interference lines, depends on the selection of the mirror. The similar reflectivities of the mirror and the specimen will give higher and greater contrast of the interference lines. Interference fringes can be produced either with monochromatic or with white light. The fringe width and interfringe distance can be varied by adjusting the two knurled screws provided with the instrument(81).

Measurement and Evaluation

A scratch is made on the coatings by means of a diamond stylus to crete a step in the coating. When fringes were obtained across the scratch certain deflection of the fringes is observed. The fringes were aligned perpendicular to the step with knurled screws provided in the interference equipment. The optimum fringe width was obtained by suitable adjustments.

Photographs are taken for each scratch at many points along the length. 8 to 9 photographs for each sample were taken to get an averaged value during measurements. The fringe deflection and interfringe distance were measured on these photographs with the help of a travelling microscope.

The following equation applies to the relationship of fringe deflection and height difference t (in air)

$$t = k \cdot \frac{\lambda}{2} \qquad (2)$$

t = height difference in nm (thickness of the film)

k = the fringe deflection in units of inter-fringe distance

λ = wavelength in nm

(546 nm. Green filter was used for the present work).

Incidentally,it is possible to differentiate the protrusions and indentations. When slight pressure is applied on the specimen stage; in case of protrusions the interference fringes migrate in opposite direction of the fringe deflection. In case of indentations the slight pressure on the specimen stage causes the fringes to migrate in the direction of the fringe deflection.

II.2.3 **Thermal Analysis**

This analysis was carried out to confirm the X-ray data on phase changes. However this could only be done on bulk powder and not on coatings. The differential thermal analysis and thermogravimetric analysis of the unstabilized ZrO_2 bulk gel is done upto 1080^{o}C using a DTA cum TG (LINSEIS, L81

Thermobalance) setup. The heating rate was 5°C/min and chart speed was 5 cm/hr. The full scale of TG was 25 mg. Both the experiments were carried out in an open air atmosphere.

II.2.4 Phase Analysis

Phase analysis is done for the ZrO_2 coatings and powders treated at different temperatures by X-ray diffraction technique. Unstabilized powder and coatings were examined after heating for 2.5 hrs at 260, 325, 450, 625, 900 and 1250°C. The stabilized powders were examined after holding at 1250°C for 2.5, 3.5 and 5 hrs.

The X-ray diffraction patterns of the coatings and the powders are obtained by using a X-ray diffractometer (Rich Seifert Iso-Debyefley 20020). CuK_α (λ = 1.5405 °A) radiation is used with a monochromator.

The substrates with the coatings are placed in a perspex holder and are fixed with a small amount of plasticine. The specimen is made horizontal by pressing it down with the help of a glass slide.

The powder specimens are prepared by spreading the powder evenly on the surface of a glass slide with the help of one or two drops of acetone, so that the powder would stick to the glass slide.

The X-ray diffraction plots (Intensity Vs. 2θ) of the samples are taken between 25° - 70° in 2θ range. The conditions of operation are as follows:

Scanning speed	1.2°/min
Chart speed	30 mm/min

Time constant	10 sec
Current voltage	20 mA, 30 kV
Counts per sec	200 - 1000

The '2θ' values corresponding to the appearance of peaks are noted from the diffraction patterns. The interplanar spacing 'd' is calculated by using the Bragg's law

$$n\lambda = 2d \sin\theta$$

where n = order of reflection = 1

λ = wavelength of the radiation used

d = interplanar spacing

θ = diffraction angle.

The relative intensities of the peaks are also measured with reference to a maximum peak which is termed as 100% peak.

The calculated 'd' values and the corresponding relative intensities are compared with the standard data available for the determination of the phase/phases present.

II.2.5 **Scanning Electron Microscopy of the Coatings**

The coatings were observed in a JEOL Scanning Electron Microscope (JSM 840A, Japan). For all the thicknesses of the coatings treated at different annealing times, micrographs are taken at a magnification of 20,000X. Care is taken to print at equal enlargement. It was found that the coating became discontinuous and its grain size increased after heat treatment at 1250^{o}C. The SEM photographs were used to measure the grain sizes and the porosity (i.e. the area from which the film has shrunk away).

II.2.5.a **Porosity Measurement by Point Analysis Method**

For porosity measurement by point analysis method[82] a square of the size 4 cm x 4 cm with a small square grid of size 0.5 cm is drawn on a transparency paper using a marker pen. This paper is placed randomly onto the photomicrograph and the number of grid intersections falling on the porosity are counted. Porosity is the black region between the grains in the photographs. The total number of grid intersections are 49 within the square. The ratio of the counted points to the total number of grid points gives the fraction of the porosity present in the corresponding coatings. This process is repeated for a number of times (25-30) for each micrograph and the average value is noted.

II.2.5.b **Grain Size Measurement**

The SEM micrographs used for porosity measurement are again used for grain size measurement by quantitative metallography methods.

Five straight lines of 4 cm length are drawn randomly without intersecting each other on a transparency paper with a marker pen. This paper is placed on the photomicrograph of a coating. The number of grains cutting each straightline are counted and the average grains per unit length is found. The transparency is changed from its initial position and again the average grains per unit length (N_L) is found. The average of such 4 or 5 readings is taken and noted as N_L.

Similarly by using the drawn squares of different sides on the transparency, the average number of grains per unit area

(N_A) are found.

Assuming a thin circular plate shape of the grains the grain size 'r' is calculated by the following formula(83)

$$r = \frac{N_L}{N_A} \qquad (3)$$

This formula is valid for the case when $t << r$

where

r = radius 'r'

t = thickness

N_L = average number of grains per unit length

N_A = average number of grains per unit area

For very large size grains where porosity was nearly equal to zero, the following relation is used for the calculation of the grain size

$$d = \frac{1.5}{N_L} \qquad (4)$$

where

d = diameter of the grain.

II.2.6 **Determination of Optical Band Gap Energy**

Absorption spectra of wide gap dielectrics or semiconductors is studied for the assessment of energy band structure. If the incident photon energy $h\nu \geq E_g$ (energy band gap) then photon absorption takes place. The energy is absorbed for the electronic transition from the valence to the conduction band. Photons with energy less than the band gap

energy are transmitted without being absorbed. The fundamental absorption edge is the energy level above which the photon absorption increases exponentially. The shape and position of the absorption edge provides much of the information about the character of the electronic transitions from the valence band to the conduction band. The electronic transitions which produce an absorption edge may be either direct or indirect. This depends on whether electrons occupy states in the valence band or the empty states are available at the bottom of the conduction band. Direct transition takes place when minima of conduction band and maxima of valence band lie at a same wave vector ('K'). However another kind of transition can also take place with the help of a phonon when two extrema are at different K's; termed as indirect transition.

Usually one measures transmittance (also absorptance or optical density) or reflectance to determine band gap value. When light is incident on a homogeneous medium, part of it is transmitted, part of it is reflected and part of it is absorbed. The transmittance (T); reflectance (R) and absorptance (D_o) denote the extent of each of above phenomena respectively. Lambart[84] has given an expression for the fall of intensity of an incident monochromatic light on a homogeneous medium with the thickness

$$I_t = I_o \cdot \exp(-kt) \qquad (5)$$

I_t = Intensity of the transmitted light

I_o = Incident intensity

k = Absorption coefficient

t = Thickness

Transmittance (T) is measured as $T = \frac{I_t}{I_o}$ (6)

Absorptance (D_o) also known as optical density is related to transmittance as shown below:

$$D_o = \log (1/T) = - \log T \quad (7)$$

T = Transmittance; D_o = Optical density.

Reflectance $R = 1 - (D_o + T)$ (8)

as $R + D_o + T = 1$

The absorption coefficient (k) as a function of photon energy is calculated using the formula[85]

$$k = \frac{D_o \times 2.303}{t} \quad (9)$$

where

D_o = optical density

Contribution from the reflection is neglected while considering the eq. (9) as absorption inccreases exponentially near band edge.

The Fan's formula[86] gives the relation between k and E_g

$$k \text{ (direct)} = A (h\nu - E_g)^{1/2} \quad (10)$$

or $k^2h^2\nu^2 = A^2h^2\nu^2 (h\nu - E_g)$

where

A = Constant

E_g = Direct energy gap.

Hence, for k = 0, $h\nu = E_g$

It can be seen that the extrapolation to k = 0 in the $(kh\nu)^2$ Vs. $h\nu$ graph gives the value of band gap energy from the above formula.

An UV-visible spectrophotometer (Schimadzu UN-160, Japan)ıs used to obtain the transmittance and/or optical density Vs. wavelength spectrum of the four different thickness samples. After dipping each time one specific side of the sample is wiped off to have coatings on only one side. The one side coated substrate after drying and baking at 600°C for 2-3 min is lowered ınto the cell and is arranged perpendicular to the beam wıth the help of a cellophane tape attached to it. For the reference, a blank uncoated sapphire substrate is used. The spectrum of absorptance Vs. wavelength is obtained for the wavelengths between 200-900 nm for all the four thickness coatings on sapphire substrates.

CHAPTER III

RESULTS AND DISCUSSION

III.1 Substrate Inluence on the Coating Thickness

To study the substrate influence on the coatıng thickness, glass slides and sapphire substrates are used. These substrates are dipped in the same sol for a number of times with an intermediate drying in the oven at 50°C for 10 min. The coating thickness after drying for 24 hrs in the oven is calculated by knowing the, weights before and after the coating, and the area of coated portion. The results are given in the Table III.1 and Table III.2.

These results are expected to be low because the coatings are assumed to be fully dense, while the actual density is likely to be less than 50% of the theoretical density. The thickness values obtained by this method are not very accurate, but will serve the purpose to get an idea how the thickness varies with each dipping and with the change of substrate.

The above results are plotted in Fig. III.1. It is shown that the coating thickness varies linearly with the number of dips. For the same number of dips the coating thickness on glass slıdes is higher than that on the sapphire substrate. It shows that wetting of zirconia on glass slide is better than that on a sapphire substrate.

Table III.2

Thickness of the Coatings on Sapphire Substrates

No. of times dip coated	Wt. of the substrate before coating (A) gm	Wt. of the coated substrate after drying at 50°C for 25 hrs B (gm)	Wt.of the coating (A-B) gm	Dimensions of the coated portion of the substrate l(cm)	b(cm)	t(cm)	Total area of the coating 2(lb)+bt+2(lt)	Thickness = Mass / Density*xArea nm
1.	0.24555	0.2456	$5x10^{-5}$	0.85	1.0	0.05	1.835	49
2.	0.6309	0.6313	$4x10^{-4}$	0.90	1.30	0.1	2.65	270
3.	0.59495	0.59555	$6.0x10^{-4}$	0.85	1.2	0.1	2.33	460

* Density of the ZrO_2 = 5.6 gm/cc.

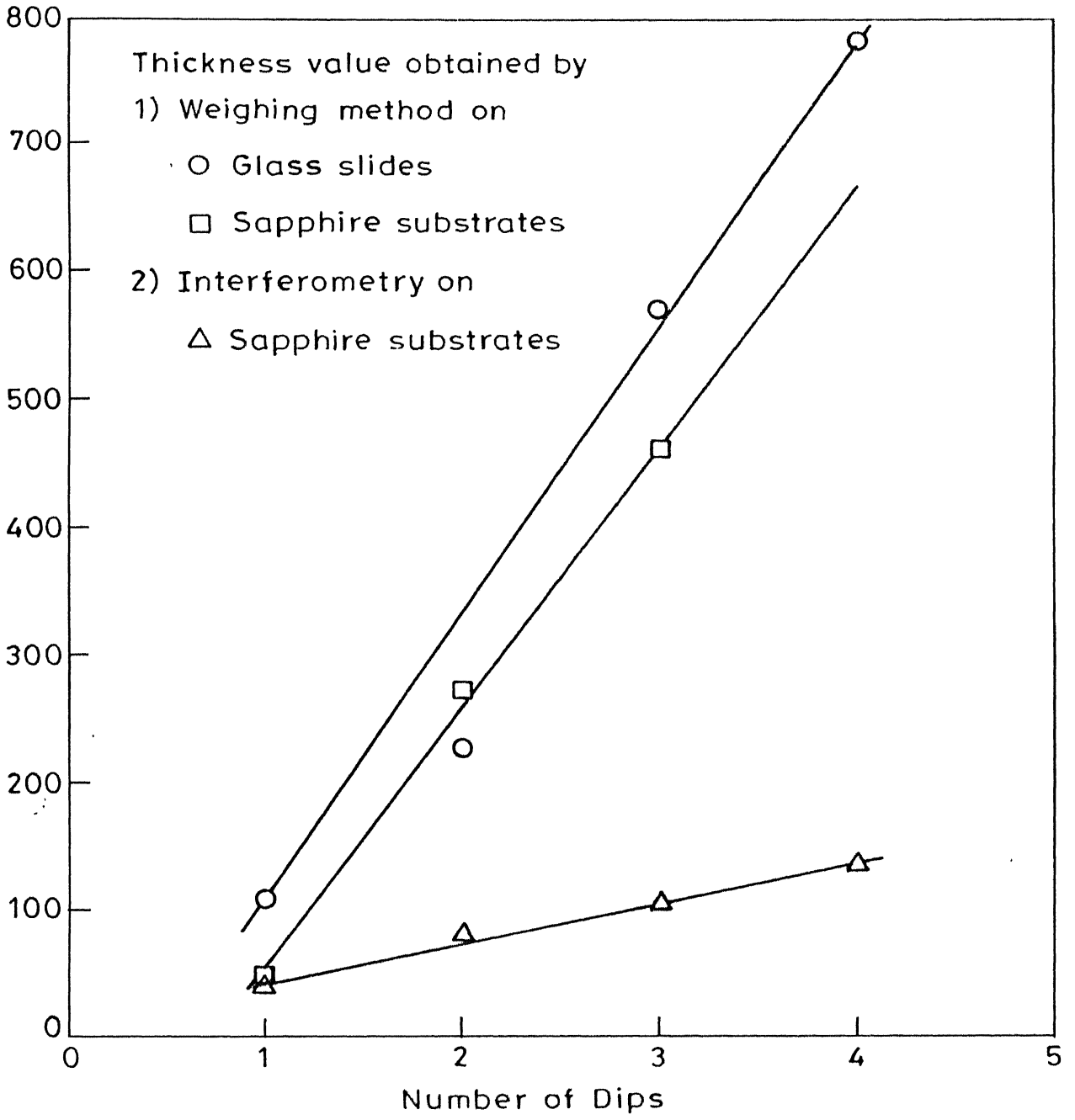

Fig. III.1 Variation of thickness of the coatings with the number of dips.

III.2 Optical Examination of the Coatings

Zirconia coatings of four different thicknesses are examined. Fig. III.2 shows schematically the regions that exist on a coated substrate. The uncoated portion is used for holding the substrate while dipping. The boundary region is of higher thickness than the coated portion as shown in Fig. III.3(a). The middle region is of sufficiently uniform thickness. The trouble zone in the lower portion is always present. This region is highly inhomogeneous and also of higher thickness, than the middle region. This can be observed visually as the lower portion is less transparent than the middle region.

Since the coatings are transparent, often the structure of the substrate is also seen while observing the coatings. The spots observed on the coatings are basically coming from the substrate. This can be seen in Fig. III.3(a). Fig. III.3(b) to Fig.III.3(m) show the photomicrographs of the four different thickness coatings namely 41 mm, 86 nm, 105 nm, 137 nm respectively. The details are given beneath each photograph.

It can be seen that the dried coatings are completely crack free for the coatings of thicknesses 41 nm and 86 nm. The cracks are slowly forming for the higher thicknesses. but they are negligible. The middle region is rephotographed after baking, and shows the cracks formed for all coatings except for 41 nm thickness coating. The extent of cracking increased with increase of thickness. The lower region which is always of higher thickness than the middle region formed by dripping of the sol,showed more severe cracking after baking treatment. So

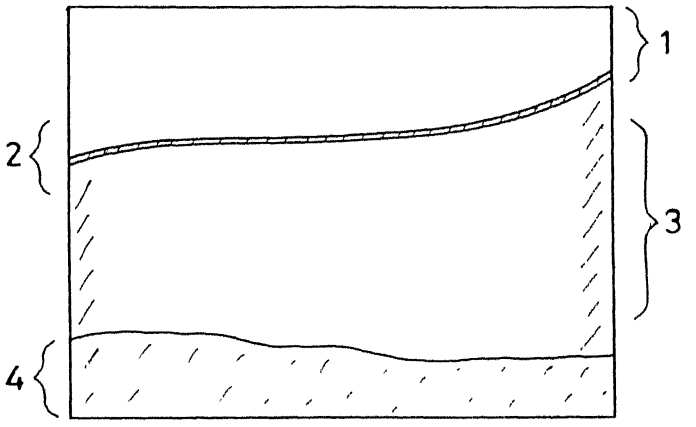

1 Uncoated portion
2. Boundary
3. Middle region having nearly uniform thickness
4. Lower portion (trouble zone)

Fig. III.2 Schematic representation of the coating as seen by the naked eye.

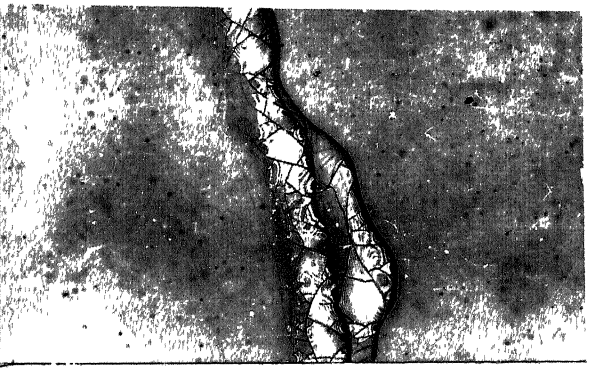

g.III.3(a) Boundary of the coating

Fig.III.3(b) Middle Region before Baking (t = 41 nm)

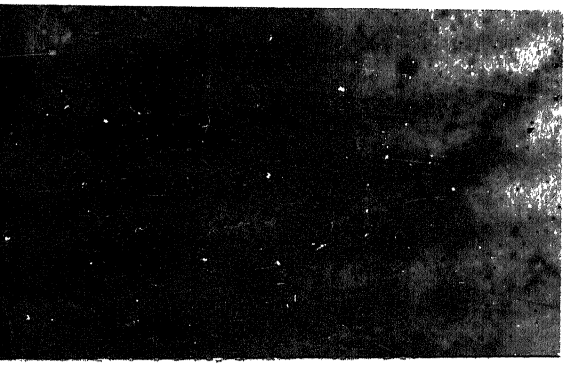

g.III.3(c) Middle Region after Baking (t=41 nm)

Fig.III.3(d) Lower Portion Before Baking (t = 41 nm)

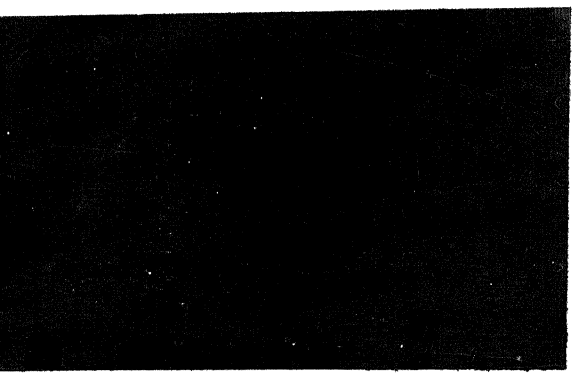

g.III.3(e) Middle Region before Baking (t = 86 nm)

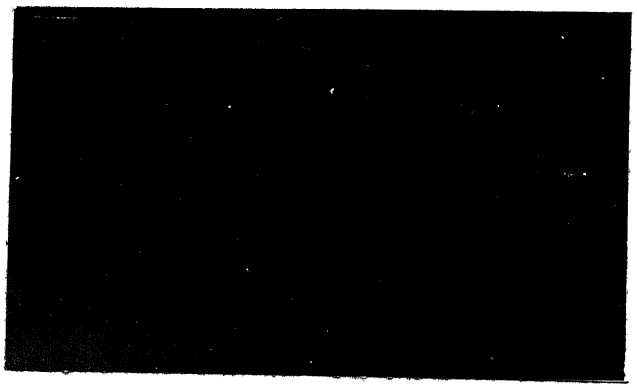

Fig.III.3(f) Middle Region after Baking (t = 86 nm)

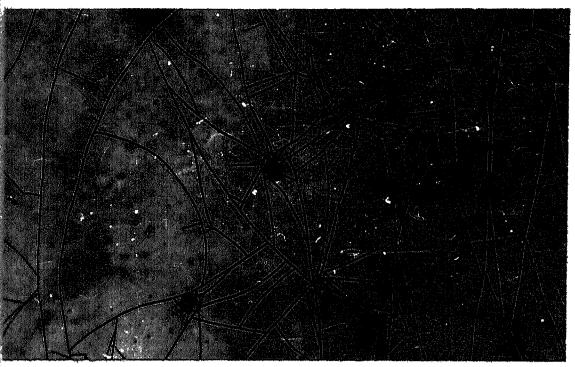

.III.3(g) Lower Portion, after Baking (t = 86 nm)

Fig.III.3(h) Middle Region before Baking (t = 105 nm)

.III.3(i) Middle Region after baking (t = 105 nm)

Fig.III.3(j) Lower Portion after Baking (t = 105 nm)

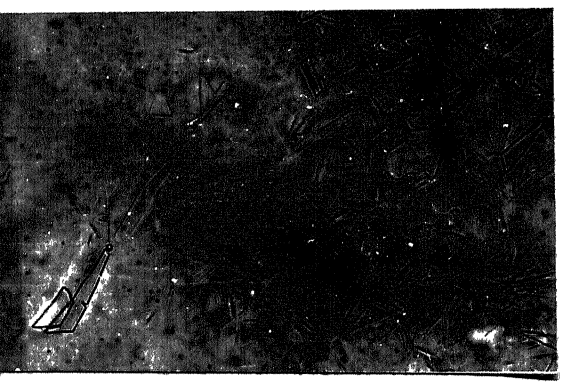

III.3(k) Middle Region before

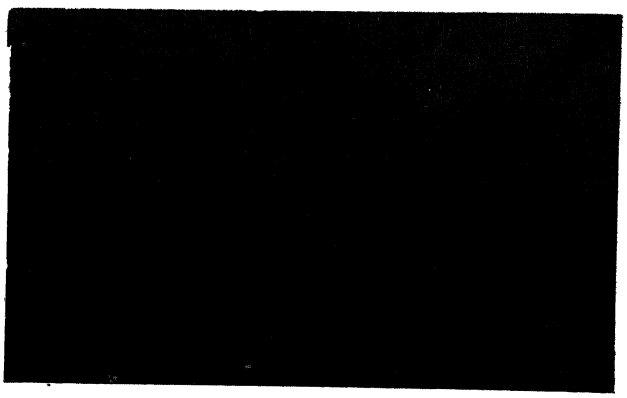

Fig.III.3(l) Middle Region after

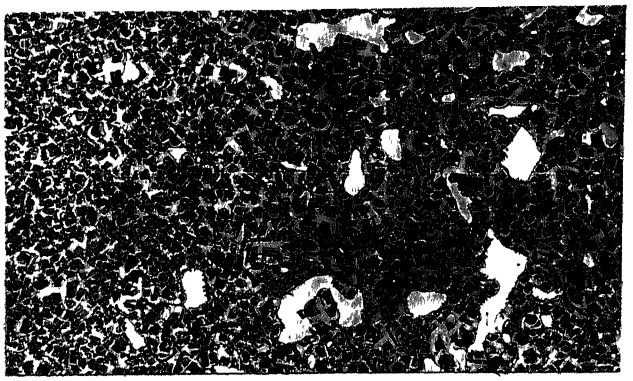

Fig. III.3(m) Lower Portion after Baking (t=137 nm)

with the increase of temperature, which introduces the thermal stresses the cracking of coatings take place. The stresses are two dimensional in the lower thickness coating and it can sustain the stresses without cracking. The combination of high temperature and high thickness results in severe cracking of the coating as shown in Fig. III.3(m). For the thickness measurements by interferometer the same baked samples are used and care was taken to focus only the middle regions of the coatings while taking the measurements.

III.3 Thickness Measurements

III.3.a Profilometry

The profilometer readings on the ZrO_2 coatings treated at 1250°C are given in Table III.3. Sample I is once coated and Sample IV is four times coated. The above readings show that the film is having different regions of the thickness. This is because after the treatment at 1250°C the film breaks and forms into distinct islands of different thicknesses. Taking averages of many readings the thickness values obtained are as follows:

		Thickness
Sample I	=	116 nm
Sample IV	=	340 nm

III.3.b Double Beam Interferometry

These measurements are taken on coatings baked at 600°C where they would not break into form islands. The values are shown in the Table III.4.

Table III.3

Thickess of Coatigs by Profilometer

Sample 1		Sample 4	
Lower portion of the coating thickness (μm)	Upper portion of the coating thickness (μm)	Lower portion of the coating thickness (μm)	Upper portion of the coating thickness (μm)
0.23	0.22	0.16	0.29
0.124	0.084	0.18	0.14
0.1335	0.12	0.12	0.36
0.233	0.083	0.762	0.40
0.204	0.077	0.11	0.23
0.11	0.063	1.07	0.3
0.145	0.127	0.38	0.39
0.22	0.014	0.25	0.21
	0.096	0.47	0.28
	0.106	0.16	0.59
	0.051	0.18	0.24
	0.0425	0.35	0.27
	0.054	0.67	0.34
	0.1825	0.12	0.1
	0.0525	0.46	0.15
	0.0545		0.26
	0.085		0.89
	0.0405		
	0.04		
	0.063		
	0.0435		
	0.051		
Average thickness = 116 nm		Average thickness = 340 nm	

Table III.4

Thickness of films by double beam interferometer.

Sample	No. of times Coated	Location1 (nm)	Location2 (nm)	Thickness of the coatings (nm)
Sample 1	Once	46	36	41
Sample 2	Twice	92	80	86
Sample 3	Thrice	107	103	105
Sample 4	Four times	133	141	137

By comparing the above two results it is clear that the profilometer readings are high. But the close examination of the profilometer readings would reveal that 50% of them fall in the lower range of values which corresponds to the interoferometer readings. These 50% of the readings must have been taken on the uniform thickness film and the higher values near the islands. The fringes and their displacements for different thickness coatings are shown in Fig.III.4(a) and (b) using which the measurements have been made. The values are plotted as thickness of the coatings Vs. number of dips in the Fig. III.1 and it is shown that they vary linearly with the number of dips.

III.4 **Thermal Analysis**

The differential thermal analysis and thermal gravimetric analysis of the unstabilized gel derived ZrO_2 powder in air was carried out upto 1080°C. The results are shown in Fig. III.5. The prominent endothermic peak at 110°C shows the desorption of physically adsorbed water and alcohol. The exothermic combustion of carbon is indicated by a sharp exothermic peak at 344°C. The crystallization information is not clearly obtained. Though the broad exotherm after 630°C gives clue to the formation of definite phase, it can not be said with certainity. The X-ray phase analyses showed the presence of cubic and tetragonal phases after 450°C heat treatment (See Fig.III.8). With this background information we can say that the broad exotherm indicates the glass to ceramic conversion. The endothermic peak which started appearing after 900°C may be dueto a t → m transformation. The T.G. plot

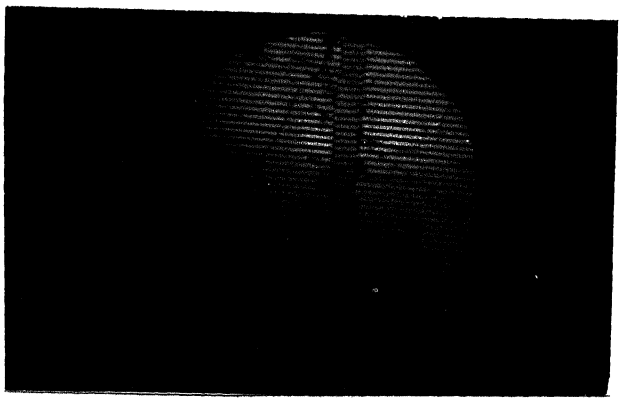

Fig. III.4(a) Sample 2, (t = 86 nm)

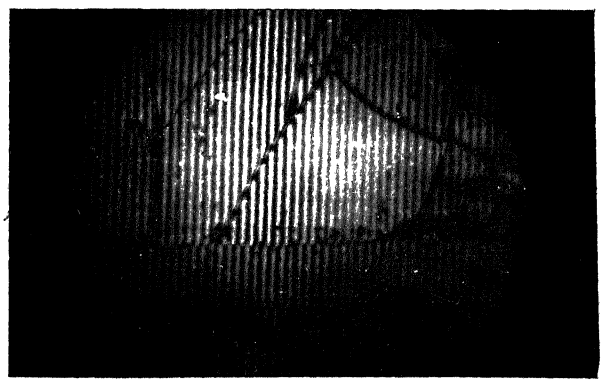

Fig. III.4(b) Sample 4, (t = 137 nm)

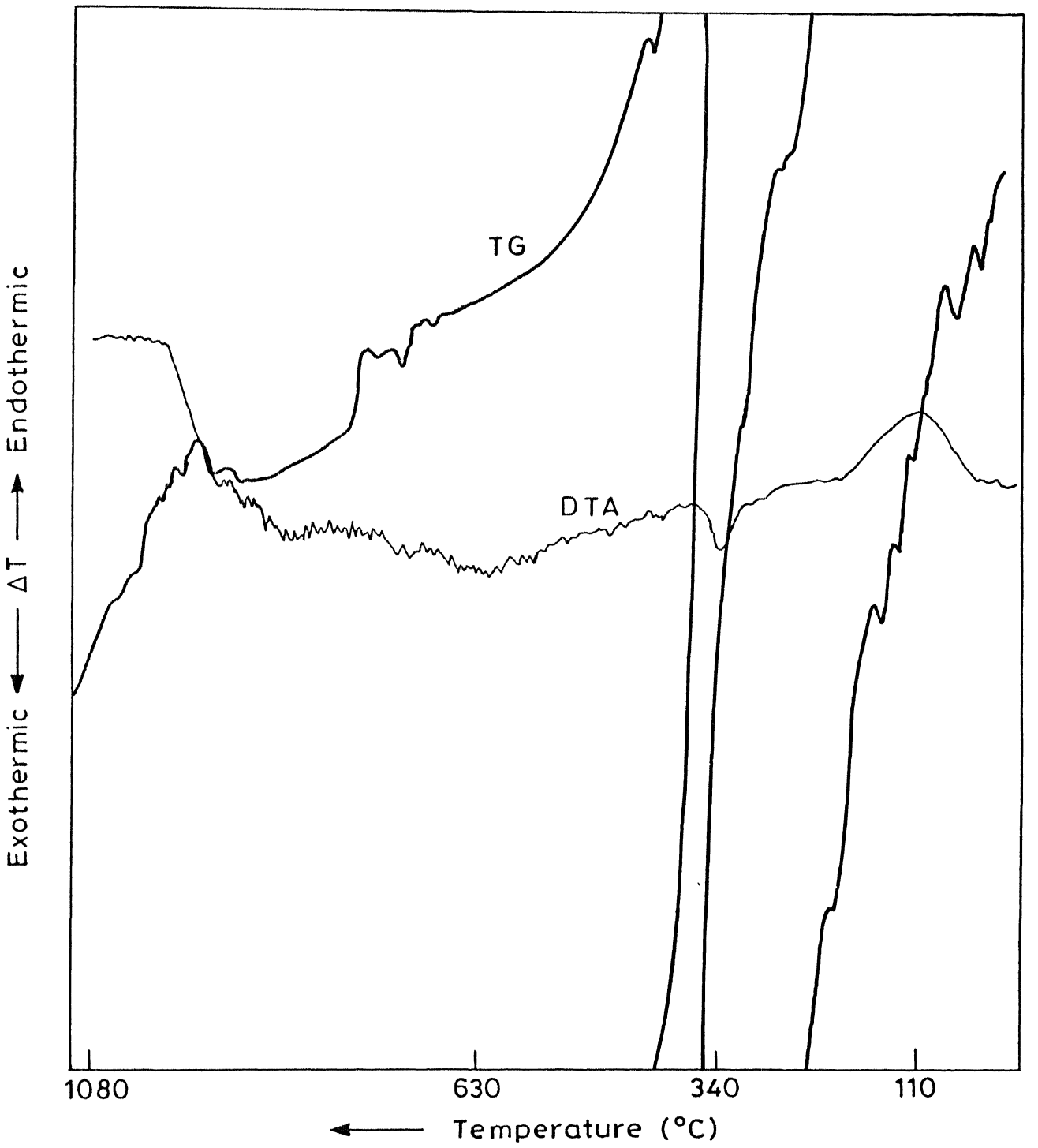

Fig. III.5 DTA and TG plots of unstabilized ZrO_2 gel powder.

confirms the DTA information by showing a drastic weight loss at 110°C (due to loss of water) and at 390°C (due to loss of carbon).

III.5 Phase Analysis

III.5.a Unstabilized Zirconia

The standard X-ray data for tetragonal, monoclinic, and cubic phases of zirconia are given in Tables III.5, III.6 and III.7 respectively. The X-ray data for α-Al_2O_3, the substrate is also given in Table III.8. While taking diffraction pattern of the coatings, often peaks corresponding to the substrate also appear. Since the substrate used is a single crystal sapphire (α-Al_2O_3) only a single peak appears. Fig. III.6(b) shows the X-ray diffraction peak coming from the substrate. Only $(11\bar{2}0)$ (or (110) in Miller indices system) planes took part in diffraction. While studying the X-ray diffraction pattern of the coatings on these substrates, this peak is ignored.

The ZrO_2 coatings as well as the gel derived ZrO_2 powders are investigated for the phases present after different heat treatments. A coating dried in air at 55°C showed no peaks indicating that it is amorphous. Coatings treated at 60°C, 325°C for 2.5 hrs also showed no crystallization. At higher temperature heat treatments, different phases appeared.

Figure III.6(a) gives the X-ray diffraction pattern for ZrO_2 coating on glass substrates treated at 450°C for 2.5 The calculated 'd' values and the phases present are given Table III.9 along with the relative intensities of the

Table III.5
ASTM Data for Tetragonal Zirconia Corrected For Room Temperature[87]

a = 5.091 A^{o}

c = 5.200 A^{o}

d(A^{o})	2θ (degrees)	I/I_{o}	hkl
2.960	30.16	100	111
2.600	34.46	18	002
2.545	35.23	25	200
2.108	42.86	6	112
1.819	50.1	65	202
1.800	50.67	35	220
1.701	53.85	2	221
1.562	59.09	25	113
1.538	60.1	45	131
1.480	62.72	12	222
1.369	68.47	2	132
1.363	68.82	2	231
1.300	72.67	4	004
1.273	74.46	8	400
1.223	78.06	2	114
1.200	79.86	2	330
1.180	81.5	12	133
1.169	82.43	8	331

Table III.6

Standard Data for Monoclinic Zirconia[88]

a = 5.1463 A^{o}
b = 5.2135 A^{o}
c = 5.3110 A^{o}
= 99.2

d(A^{o})	2θ (degrees)	I/I_{o}	hkl
3.694	24.07	18	011
3.636	25.46	12	110
3.163	28.19	100	$\bar{1}11$
2.839	31.48	64	111
2.620	34.19	22	002
2.605	34.40	12	020
2.540	35.30	14	200
2.2131	40.73	12	$\bar{2}11$
1.8480	49.26	16	022
1.8186	50.11	18	$\bar{2}20$
1.8032	50.57	12	$\bar{1}22$
1.6934	54.11	11	202,300
1.6567	55.41	12	013
1.6568	55.62	10	113

Table III.7

Standard Data for Cubic Phase Zirconia Corrected to Room Temperature[89]

a = 5.09 A^{O}

d(A^{O})	2θ (degrees)	I/I_{O}	hkl
2.93	30.48	100	111
2.55	35.16	25	200
1.801	50.64	50	220
1.534	60.28	20	311
1.471	63.15	5	222
1.270	74.67	5	400
1.167	82.60	5	331
1.135	85.47	5	420

Table III-8

Standard Data for α-Al_2O_3

10-173 MINOR CORRECTION

d	2.09	2.55	1.60	3.48	α-Al_2O_3
I/I_1	100	90	80	75	ALPHA ALUMINUM OXIDE (CORUNDUM)

Rad. $CuK\alpha_1$ λ 1.5405 Filter Ni Dia
Cut off I/I_1 DIFFRACTOMETER
Ref. NAT. BUR. STANDARDS (U.S.) CIRC. 539 9 3 (1959)

Sys. TRIGONAL SG D^6_{3d} - $R\bar{3}c$ (167)
a_o 4.758 b_o c_o 12.991 A C 2.7303
α β γ Z 6 Dx 3.987
Ref IBID.

$\varepsilon\alpha$ $n_w\beta$ $\varepsilon\gamma$ Sign
2V D mp Color
Ref

SAMPLE ANNEALED AT 1400°C FOR FOUR HOURS IN AN Al_2O_3 CRUCIBLE. SPECT. ANAL. SHOWED <0.1% K,Na,Si; <0.01% Ca, Cu, Fe,Mg,Pb; <0.001% B,Cr,Li,Mn,Ni.
CORUNDUM STRUCTURE.
PATTERN MADE AT 26°C.

d Å	I/I_1	hkl	d Å	I/I_1	hkl
3.479	75	012	1.1382	2	311
2.552	90	104	1.1255	6	312
2.379	40	110	1.1246	4	128
2.165	< 1	006	1.0988	8	0.2.10
2.085	100	113	1.0831	4	0.0.12
1.964	2	202	1.0781	6	134
1.740	45	024	1.0426	14	226
1.601	80	116	1.0175	2	402
1 546	4	211	0.9976	12	1 2..0
1 514	6	122	.9857	< 1	1.1.12
1 510	8	018	9819	4	4[illegible]4
1.404	30	124	.9431	< 1	321
1.374	50	030	.9413	<	1 2.11
1.337	2	125	.9345	4	318
1.276	4	208	.9178	4	229
1.239	16	1.0.10	.9076	14	324
1.2343	8	119	.9052	4	0 1.14
1.1898	6	220	.8991	6	410
1.1600	< 1	306	.8884	< 1	235
1.1470	6	223	PLUS 11	LINES	TO .7931

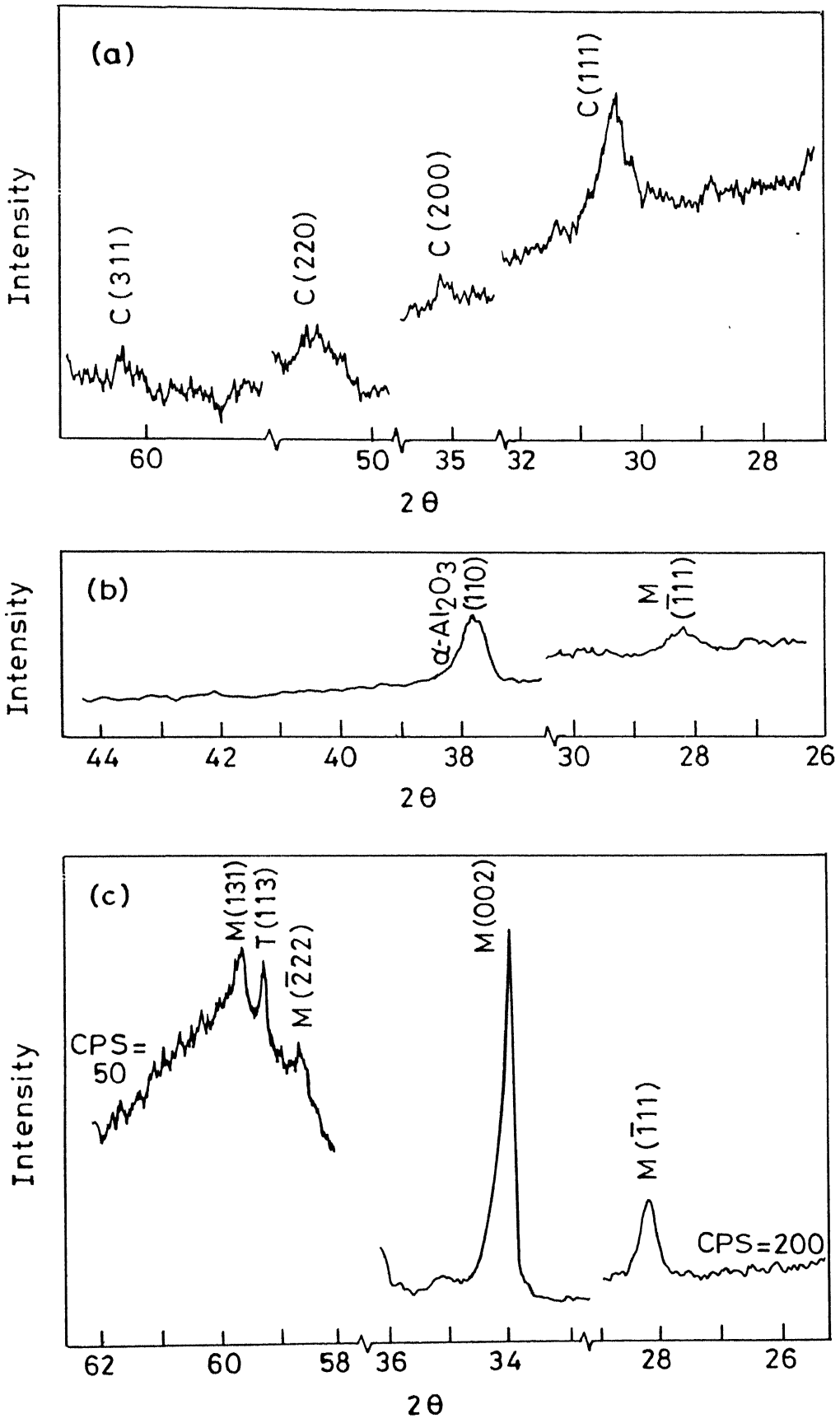

Fig. III.6 X-ray diffraction pattern of the ZrO_2 coatings treated at (a) 450°C ; (b) 900°C and (c) 1250°C for 2.5 hours. M = Monoclinic, T = Tetragonal, C = Cubic

Table III.9

X-ray data for ZrO_2 coating on glass substrate treated at 450 ^{o}C for 2.5 Hrs.

Peak No.	2θ (degrees)	d (A^{o})	I/I_o	Phases	hkl
1	30.42	2.936	100	C	111
2	35.24	2.545	54	C	200
3	50.64	1.801	21	C	220
4	60.2	1.536	18	C	311

C = Cubic

The phase present is only cubic without the tetragonal or monoclinic phases. The relative intensity of (200) reflections is high, compared to the value given in the standard Table III.7. This is due to the texture present in the coatings along (200).

The coatings treated at 625°C for 2.5 hrs also showed the presence of cubic phase. The 2θ values and calculated 'd' values are shown in Table III.10 along with the relative intensities of the peaks. The Fig. III.7(b) shows the X-ray diffraction pattern.

The coatings treated at 900°C ffor 2.5 hrs showed only one monoclinic peak (2θ = 28.18) as illustrated in Fig. III.6(b). This implies that the film has transformed to a monoclinic phase with mostly ($\bar{1}11$) orientation.

Figure III.6(c) shows the X-ray diffraction pattern of the ZrO_2 coating on sapphire, treated at 1250°C for 2 hrs. Table III.11 gives the 2θ values, calculated 'd' values, relative intensities of the peaks and the phases present. The very high intensity of the peak corresponding to (002) planes relative to the ($\bar{1}11$) planes indicates that the coatings are highly texstured along (002). The peaks observed correspond to monoclinic phase.

The above results can be compared with those for the gel derived ZrO_2 powder prepared from the same sol as used for coating. The gel derived ZrO_2 powder also showed the amorphous nature when it is treated, at 55°C for 72 hrs and 260°C, 325°C for 2.5 hrs respectively.

Table III.10

-ray data for ZrO_2 coating on Sapphire, treated at 625 ^{0}C for 2.5 Hrs.

eak No.	2Θ (degrees)	d (A^0)	I/I_0	Phases	hkl
	30.4	2.93	100	C	111
	50.8	1.795	30	C	220
	60.4	1.53	16	C	311

C = Cubic

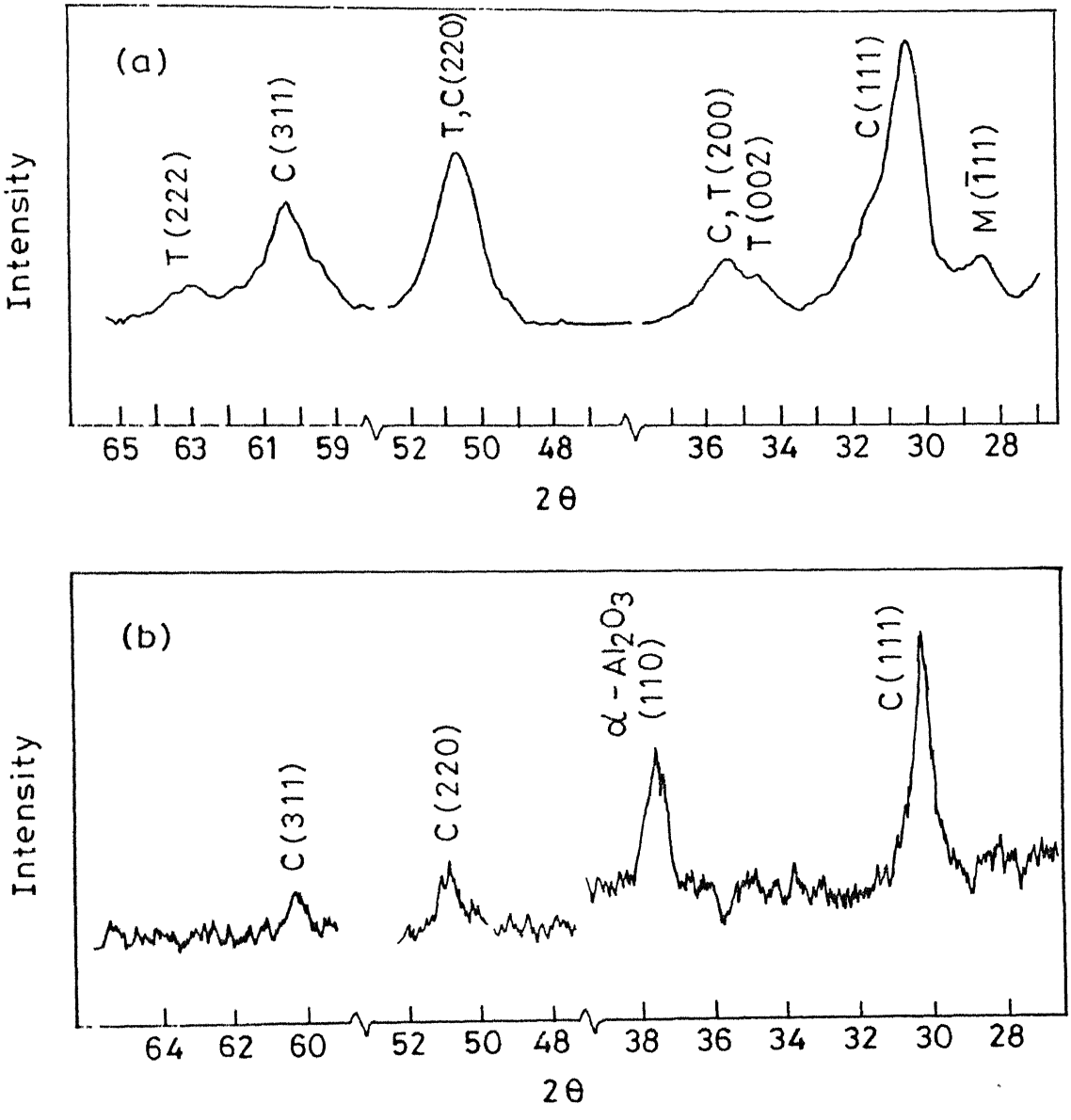

Fig. III.7 X-ray diffraction pattern of the unstabilized ZrO_2 treated at 625°C for 2.5 hrs (a) powder (b) coating. M = Monoclinic, T = Tetragonal, C = Cubic

Table III.11

X-ray data for ZrO_2 coating treated at 1250 ^{o}C for 2.5 Hrs.

Peak No.	2θ (degrees)	d (A^{o})	I/I_o	Phases	hkl
1	28.2	3.161	35	M	$\bar{1}11$
2	33.96	2.63	100	M	002
3	58.68	1.572	9	M	$\bar{2}22$
4	59.3	1.56	12	T	113
5	59.68	1.54	13	M	131

T = Tetragonal , M = Monoclinic

The X-ray data of the gel derived ZrO_2 powder treated at 450°C for 2.5 hrs is given in Table III.12. The pattern is shown in Fig. III.8(a).

The X-ray data obtained for a gel derived ZrO_2 powder treated at 625°C for 2.5 hrs is given in Table III.13. After this treatment also only cubic and/or tetragonal phases are present. The X-ray diffraction pattern is shown in Fig. III.7(a).

Figure III.8(b) shows the X-ray diffraction pattern of thus obtained ZrO_2 powder treated at 900°C for 2.5 hrs. The 2θ values, calculated 'd' values and relative intensities, phases are given in Table III.14.

The phase present is tetragonal. A few peaks corresponding to monoclinic phase are also observed. This shows that the phase transformation tetragonal to monoclinic is taking place at these temperatures. The relative intensities calculated for the peaks match with the values given in the standard Table III.5. This shows that the texture is absent, unlike in the coatings. This result is in contrast to the previous investigation that only monoclinic phase exists after 800°C, 24 hr heat treatment[59].

X-ray diffraction pattern of the gel derived ZrO_2 powder treated at 1250°C for 2.5 hrs is shown in Fig. III.8(c). The X-ray data is given in Table III.15. The phase present is completely monoclinic. The absence of texture is observed. The relative intensities of the peaks are as described by the standards.

Table III.16 gives the summary of the phase analysis of ZrO_2 coatings and powders after different heat treatments. The

Table III.12

X-ray data for gel derived ZrO_2 powder treated at 450 ^{0}C for 2.5 Hrs.

Peak No.	2θ (degrees)	d (A^0)	I/I_0	Phases	hkl
1	30.5	2.928	100	C	111
2	35.2	2.547	24	C,T	200
3	50.55	1.804	51	C,T	220
4	60.05	1.539	38	T	131
5	62.8	1.478	10	T	222

C = Cubic , T = Tetragonal

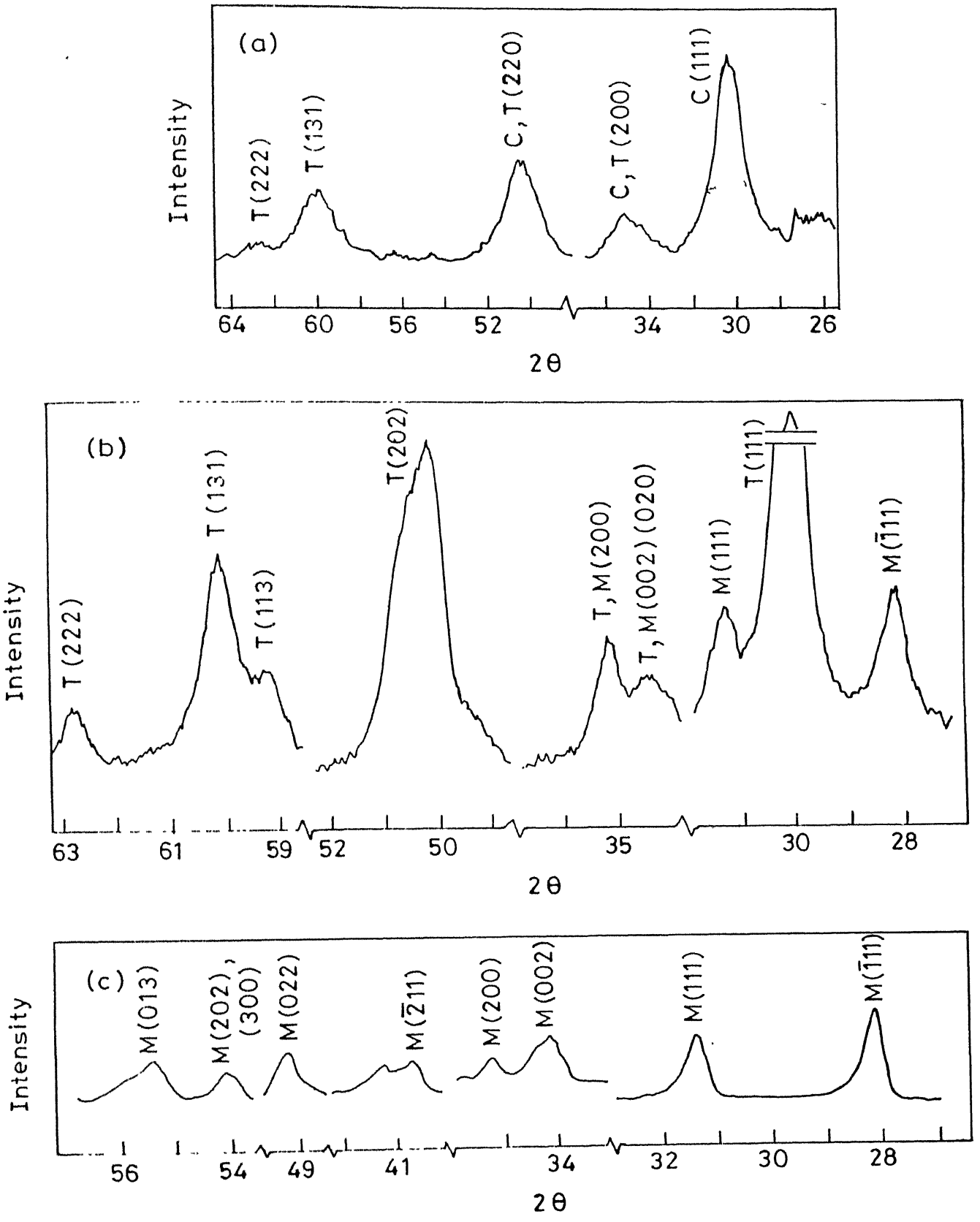

Fig. III.8 X-ray diffraction pattern of the gel derived unstabilized ZrO_2 powder treated for 2.5 hrs at (a) 450°C (b) 900°C (c) 1250°C. M = Monoclinic, T = Tetragonal, C = Cubic

Table III.13

X-ray data for gel derived ZrO_2 powder treated at 625 °C for 2.5 Hrs.

Peak No.	2θ (degrees)	d (Å)	I/I$_0$	Phases	hkl
1	28.3	3.15	28	M	$\bar{1}11$
2	30.4	2.937	100	C	111
3	34.55	2.594	19	T	002
4	35.28	2.542	29	C,T	200
5	50.55	1.804	68	C,T	220
6	60.28	1.534	47	C	311
7	62.88	1.476	14	T	222

C = Cubic , T = Tetragonal , M = Monoclinic

Table III.14

X-ray Data for Gel Derived ZrO_2 Powder Treated at $900^{o}C$ for 2.5 Hours

S.No.	2θ (degrees)	d(A^{o})	I/I_o	Phases	hkl
1.	28.2	3.16	27	M	$\bar{1}11$
2.	30.16	2.96	100	T	111
3.	31.4	2.846	25	M	111
4.	34.5	2.597	15	T,M	002,020
5.	35.2	2.547	24	T,M	200,200
6.	50.2	1.815	66	T	202
7.	59.28	1.557	17	T	113
8.	60.125	1.537	40	T	131
9.	62.8	1.48	14	T	222

M = Monoclinic

T = Tetragonal

Table III.15

X-ray Data for ZrO_2 Powder Treated at 1250°C for 2.5 hrs

S.No.	2θ (degrees)	d (A^o)	I/I_o	Phases	hkl
1.	24.04	3.698	15	M	011
2.	28.16	3.166	100	M	$\bar{1}11$
3.	31.44	2.842	69	M	111
4.	34.16	2.622	25	M	002
5.	34.36	2.607	22	M	020
6.	35.24	2.544	14	M	200
7.	40.76	2.21	17	M	$\bar{2}11$
8.	49.25	1.848	20	M	022
9.	50.14	1.81	18	M	$\bar{2}20$
10.	54.06	1.694	18	M	202,300
11.	55.4	1.657	19	M	013

M = Monoclinic

Table III.16

Phase Analysis of ZrO_2 Powder and Coatings

(Unstabilized)

S.No.	Temperature	Annealing Time	Phases detected by XRD	
			Powders	Coatings
1.	55°C	72 hrs	Amorphous	Amorphous
2.	260°C	2.5 hrs	Amorphous	Amorphous
3.	325°C	2.5 hrs	Very broad peak corresponding to cubic phase	Amorphous
4.	450°C	2.5 hrs	Cubic	Cubic
5.	625°C	2.5 hrs	Tetragonal with traces of cubic phase	Cubic
6.	900°C	2.5 hrs	Tetragonal with traces of monoclinic phase	Monoclinic
7.	1250°C	2.5 hrs	Monoclinic	Monoclinic

results show that the order amorphous - cubic - tetragonal - monoclinic is followed during heating from room temperature to 1250°C of the gel derived ZrO_2 powder. The tetragonal phase in the coatings is not observed under similar heat treating conditions. The texture of the coatings and the particle size are believed to be the reasons for this.

III.5.b Stabilized Zirconia

The doping of ZrO_2 with Y_2O_3 for the stabilization of the high temperature phase is done. Fig. III.9 shows the X-ray diffraction pattern of the 8 mole% Y_2O_3 doped, gel derived ZrO_2 powder, treated at 1250°C for 2.5, 3.5 and 5 hrs. Table III.17 gives the X-ray data for these samples. In all the three treatments similar peaks are observed. Peaks corresponding to Y_2O_3 (both hexagonal and cubic) are absent. This means that Y_2O_3 is not in excess and is not existing as a separate phase.

The results given in the Table III.17 can be compared with those of unstabilized ZrO_2 powder given in the Table III.15 for the same heat treatment. The monoclinic phase is completely absent in the Y_2O_3 doped ZrO_2. The tetragonal phase is stabilized completely.

III.6 Scanning Electron Microscopy of the Coatings

III.6.a Porosity Measurement

The as deposited film is continuous. On heating at 1250°C for increasing times, there is an increase in the grain size. In addition, bare substrate areas from where the film has shrunk away, appear. The fraction of the bare substrate area is termed percent porosity, in the film.

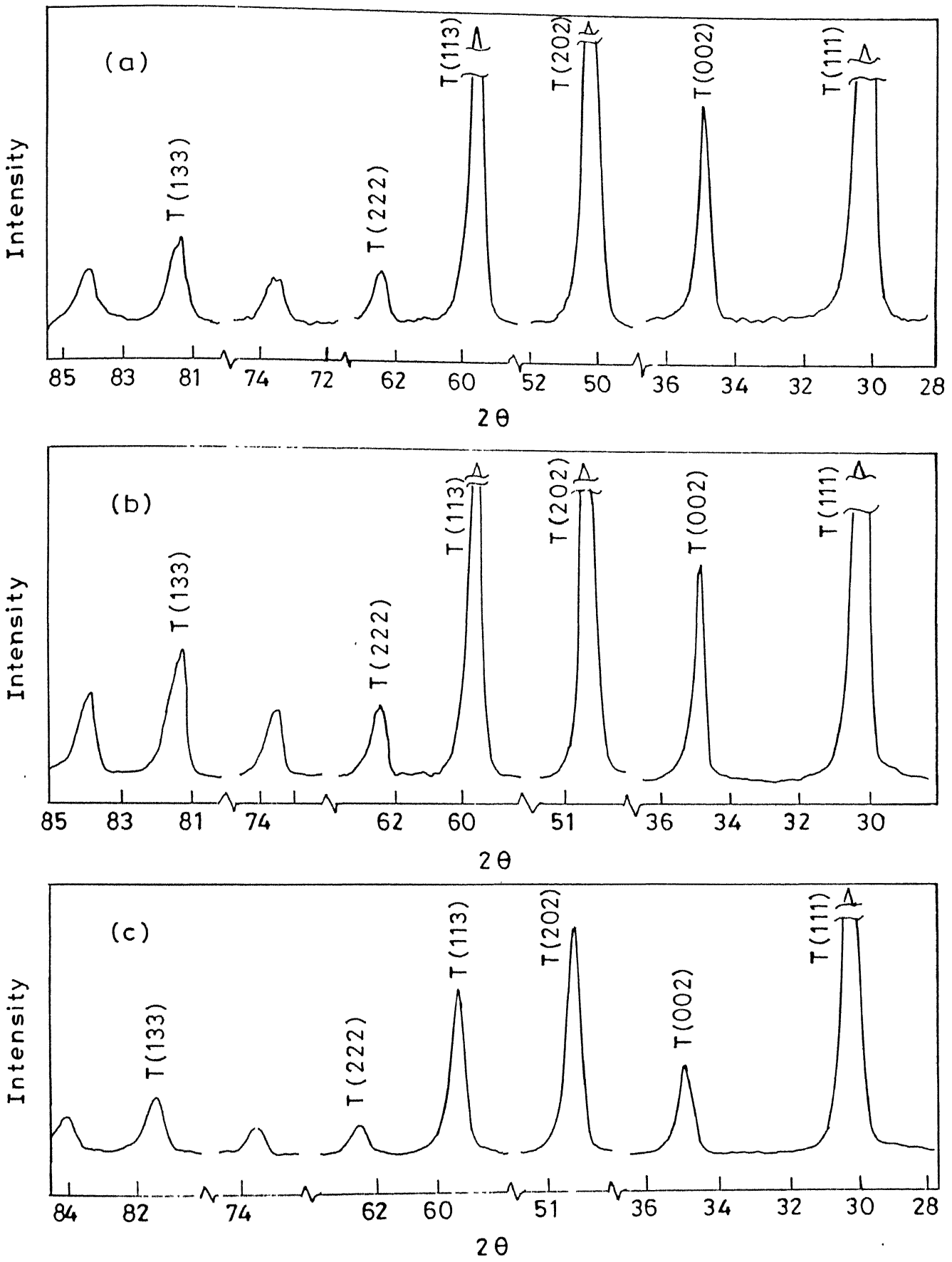

Fig. III.9 X-ray diffraction patterns of the stabilized (with 8 mole % Y_2O_3) gel derived ZrO_2 powder treated at 1250°C for (a) 2.5 hrs; (b) 3.5 hrs; (c) 5 hrs. T = Tetragonal

Table III.17

Xlray Data for Stabilized ZrO_2 Powder Treated at 1250°C for 2.5, 3.5, and 5 Hours

2.5 hrs; 1250°C			3.5 hrs; 1250°C			5 hrs; 1250°C			Phase
2θ	d	I/I_o	2θ	d	I/I_o	2θ	d	I/I_o	
30.04	2.972	100	30.1	2.966	100	30.16	2.96	100	T
34.84	2.573	24	34.88	2.57	25	34.94	2.565	23	T
50.12	1.818	55	50.12	1.818	63	50.16	1.817	58	T
59.48	1.552	34	59.52	1.528	43	59.56	1.55	43	T
62.48	1.485	5	62.48	1.485	8	62.48	1.485	7	T
73.6	1.286	4	73.52	1.287	7	73.56	1.286	6	
81.36	1.182	9	81.4	1.181	15	81.48	1.18	14	T
84.0	1.151	6	84.0	1.151	9	84.05	1.15	9	

T = Tetragonal

The porosity of the coatings as determined by point nalysis from the SEM micrographs is given in the Table III.18. ig. III.11 shows some of these SEM micrographs that are used or the measuremets. All the coatings are heat treated at 250^{o}C for the times shown in vertical columns. The porosity is iven as the percentage porosity.

These values are plotted in Fig. III.10 as percentage orosity Vs. coating thickness for all the annealing times. The orosity decreases with increase of coating thickness for the ame annealing time.

Sintering phenomenon is associated with decrease in orosity. An increase in the porosity in the present case ccurs due to poor wetting of the sapphire substrate by irconia film. The porosity first appears at triple grain junction (as shown in Fig. III.11(a)).

Figure III.12 compares the cases for good and poor wetting. A smaller value of θ, the contact angle, implies a better wetting.

Figure III.13(a) shows schematically the nucleation of cavity at the triple point between the substrate and a grain boundary.

Figure III.13(b) shows this in more detail. In (i) the pore surface is concave towards the grain and the pore will grow while in (ii) the pore surface is concave towards the pore and the pore shrinks.

Table III.18

Percentage porosity of the ZrO_2 coatings treated at 1250 ^{0}C

Sl. No.	Sample	Thickness (nm)	% porosity after heating at 1250 ^{0}c for 5 min.	30 min.	4 hrs.	8 hrs.
1	Sample 1	41	6.12	28.36	28.67	35
2	Sample 2	86	4.08	10.2	23.63	32.5
3	Sample 3	105	3.06	9.83	0	0
4	Sample 4	137	--	6.63	0	0

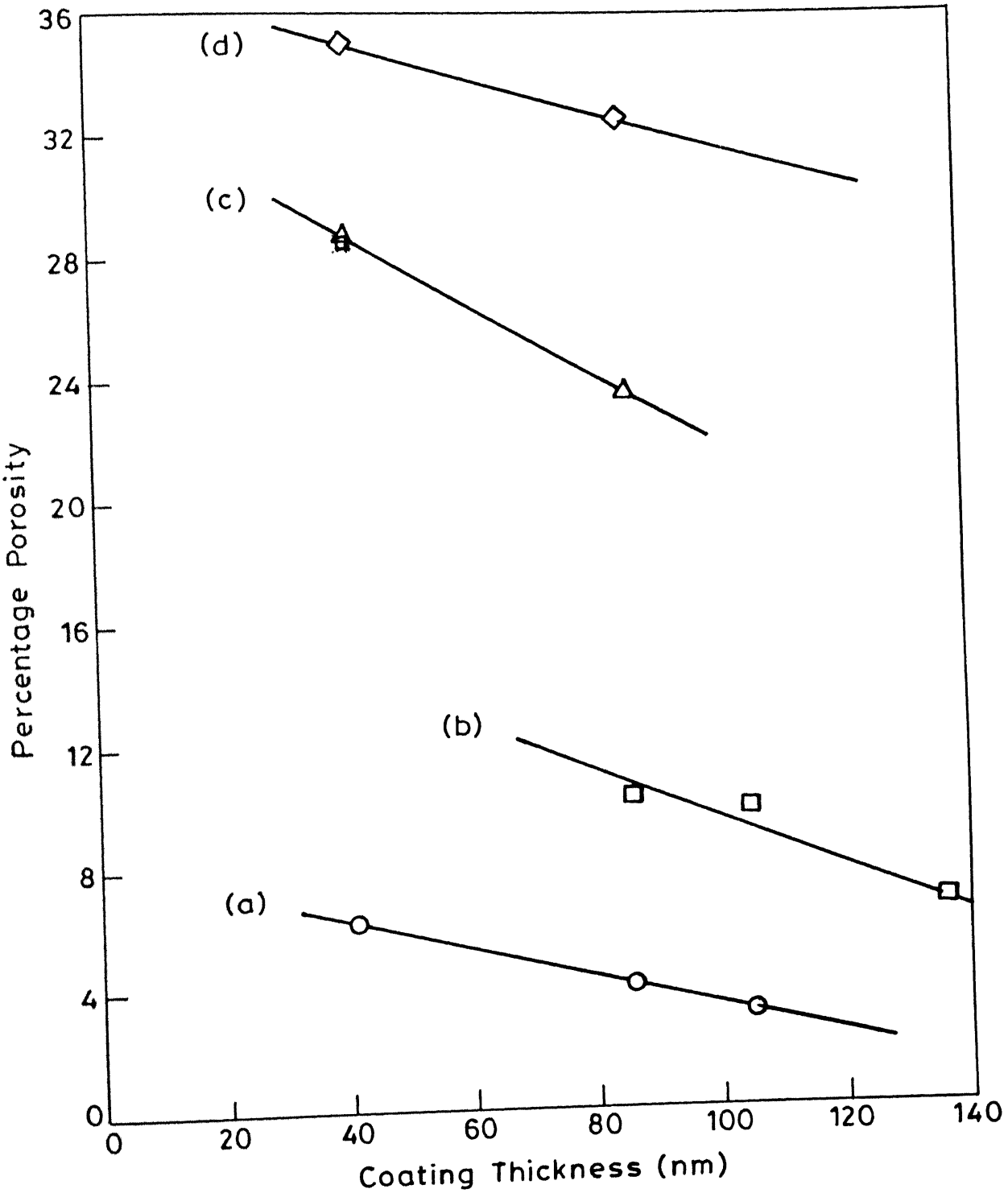

Fig. III.10 Variation of porosity with the thickness for the heat treatments at 1250°C for (a) 5 min (b) 30 min

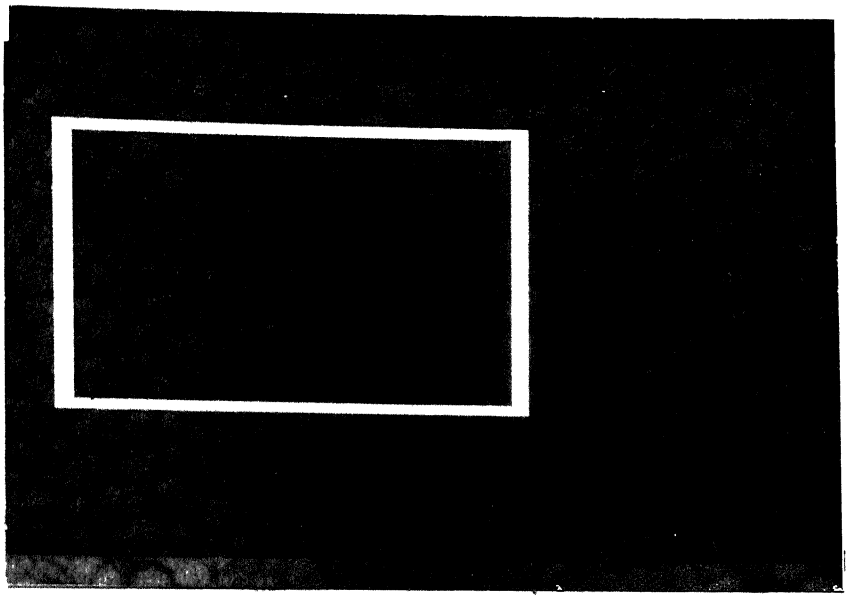

Fig.III.11(a) Sample 1, 5 min at 1250°C

1 μ

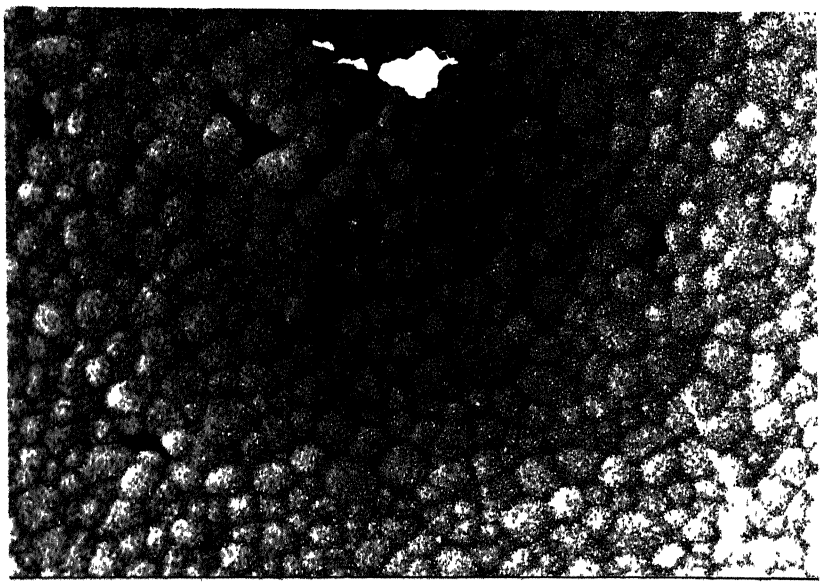

Fig.III.11(b) Sample 2, 5 min at 1250°C

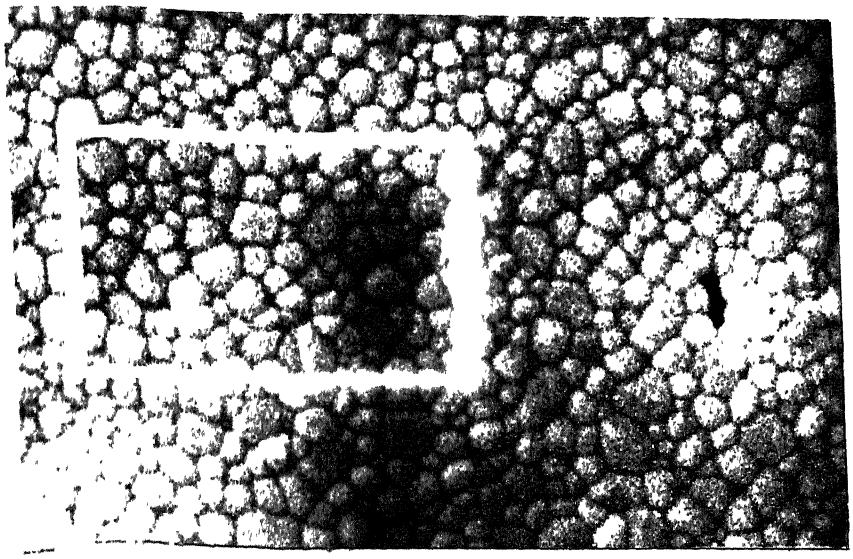

Fig. III.11(c) Sample 3, 5 min at 1250°C

1 μ

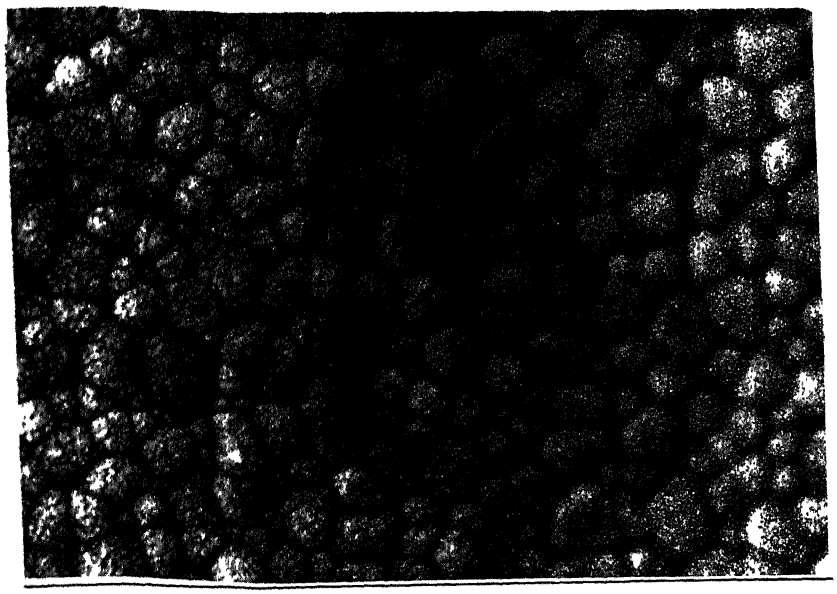

Fig.III.11(d) Sample 3, 30 min at 1250°C

Fig.III.11(e) Sample 3, 4 hrs at 1250°C

1 μm

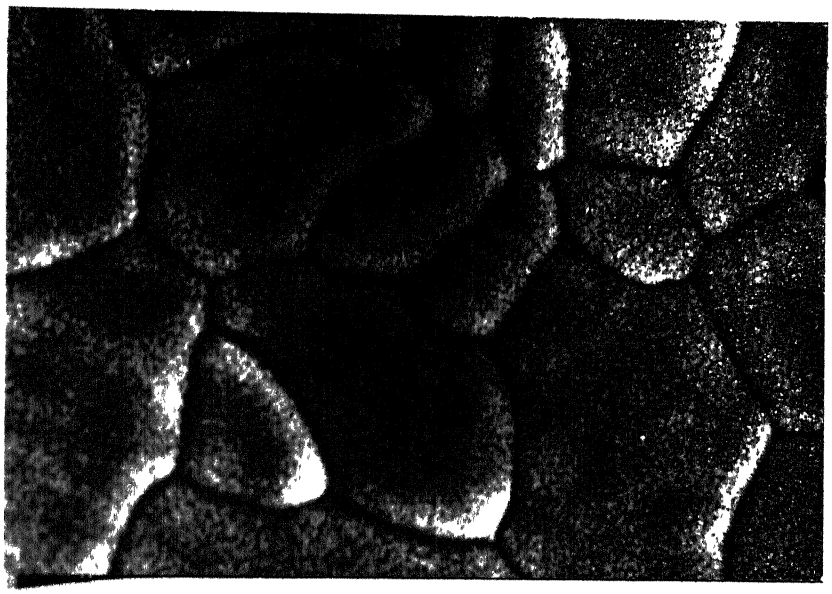

Fig.III.11(f) Sample 3, 8 hrs at 1250°C

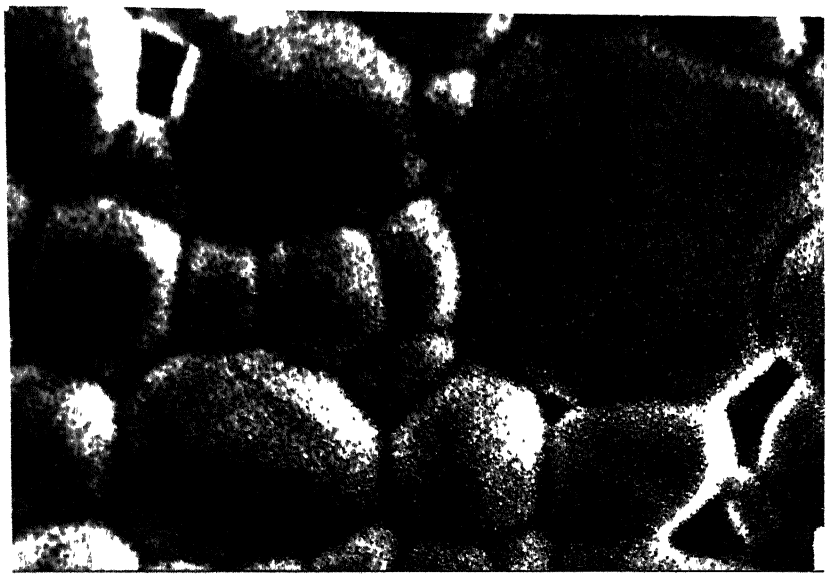

Fig.III.11(g) Sample 4, 18 hrs at 1250°C

1 μ

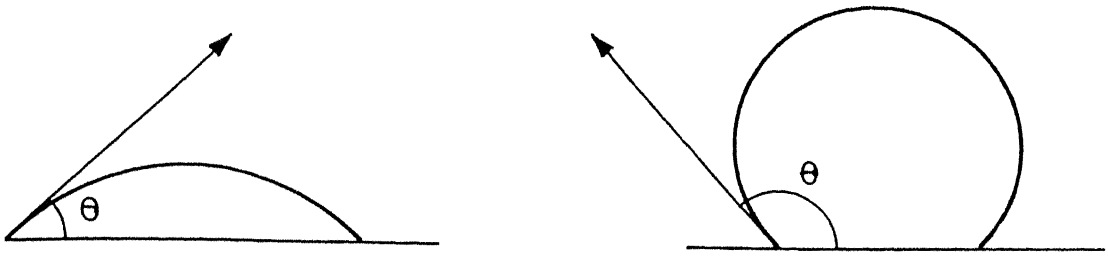

Good wetting
θ small

Poor wetting
θ large

Fig. III.12 Contact angles for two cases of wetting.

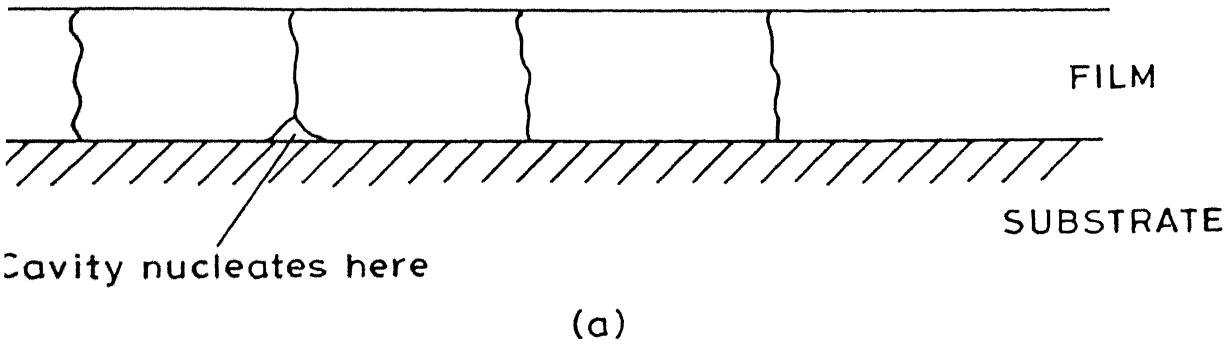

(a)

(i) (b) (ii)

Fig. III.13 Schematic diagram showing the (a) Nucleation of cavity at the triple point between the substrate and a grain boundary (b) Criteria for the stability of cavities

For Figure (i) $\alpha < \pi - (\frac{\pi}{2} + \phi)$

$$\text{i.e.} \quad \frac{\pi}{2} - \phi$$

$$\text{i.e.} < \frac{\pi}{2} - (\pi - \theta) \quad \text{i.e.} < -\frac{\pi}{2} + \theta$$

$$\text{or} \quad \theta > \frac{\pi}{2} + \alpha$$

where α = dihedral angle.

whereas for Fig. (ii)

$$\theta < \frac{\pi}{2} + \alpha .$$

Hence for the pore to grow which is the present case

$$\theta > \frac{\pi}{2} + \alpha$$

where θ is the contact angle.

For the above to apply, the grain size of the film should grow to a value equal to at least the thickness of the film, so that the film is a two dimensional film with only single grain thickness. Hence the initiation of porosity in a film should occur at longer times for thicker films. This is borne out by Fig. III.14.

Assuming that the development of porosity occurs by diffusion in a direction perpendicular to the film, the thickness of the film and time for development of a given porosity should vary as

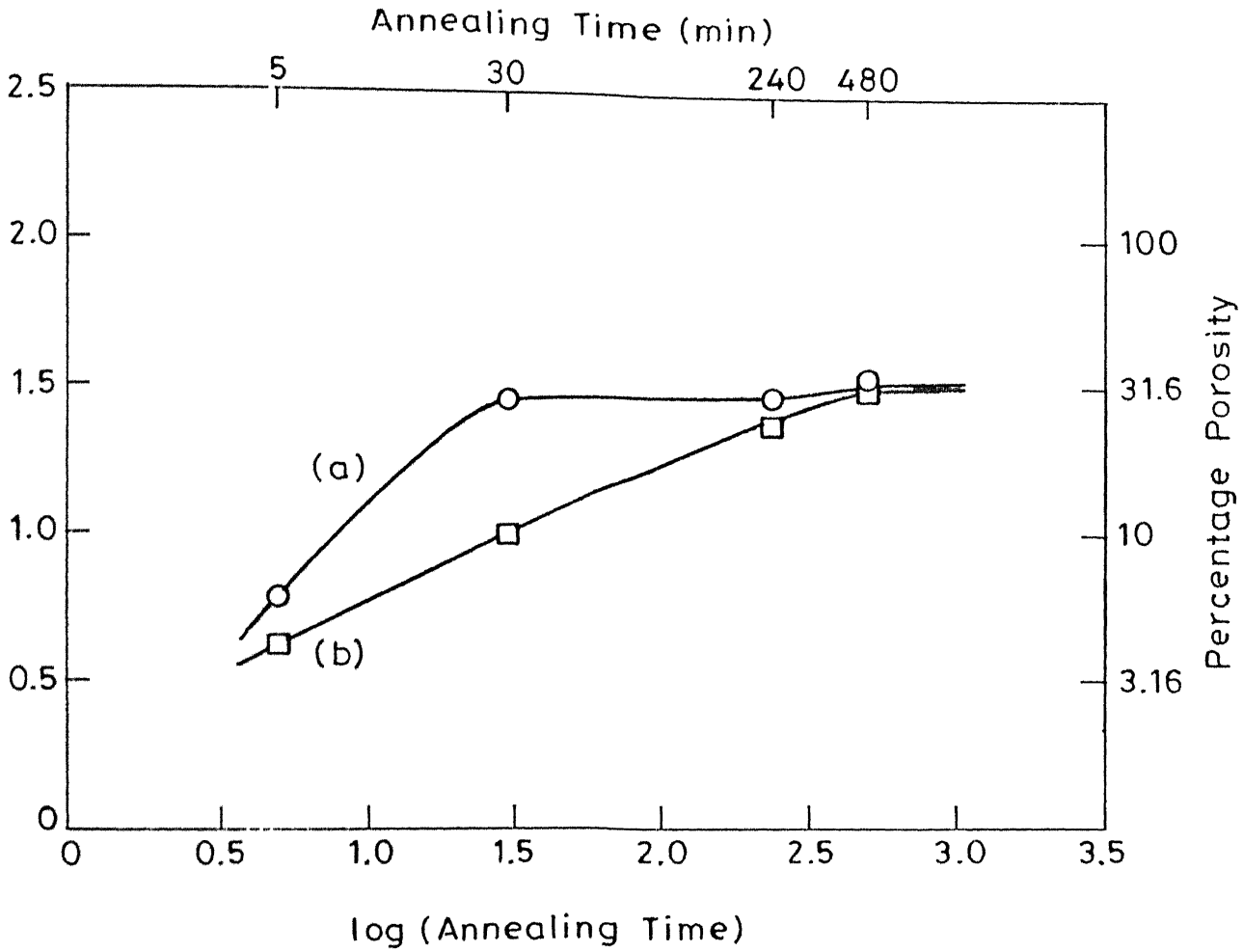

Fig. III.14 Variation of porosity with the annealing time for the thicknesses (a) 41 nm (b) 86 nm.

Thickness α $\sqrt{\text{time for a given porosity.}}$

In Fig. III.15 log (film thickness) is plotted against log (t) for a porosity of 32%. Although only two valid points are available the slope is 0.27 which is close to the expected value of 0.5.

III.6.b **Grain Size Measurement**

The grain size measurements are done using the same SEM micrographs that are used for porosity measurements. The grains are assumed to have thin plate shape with t << r where 'r' is the radius of the plate and 't' is the thickness. Results are tabulated in Tables II .19.

The grain size measurements for large grains are done by using the formula $d = \frac{1.5}{N_L}$ where N_L = number of grains per unit length and 'd' is the diameter of the grain. The assumption of plate shape does not hold for coarse grain zero porosity coatings as they no longer exist as individual disconnected particles (grains).

The log(r) Vs. log (annealing time) curves are plotted in Fig. III.16 for three different thickness coatings. The slope of the lines obtained is not constant through out the range of annealing times. There are two differents slopes observed for each thickness of the coating. The initial region has slope less than 1/2 where as the second region has higher than this. This shows that till certain annealing time the grain growth is inversely proportional to the grain size i.e. $d \propto t^{1/2}$. For longer annealing periods exaggerated grain growth

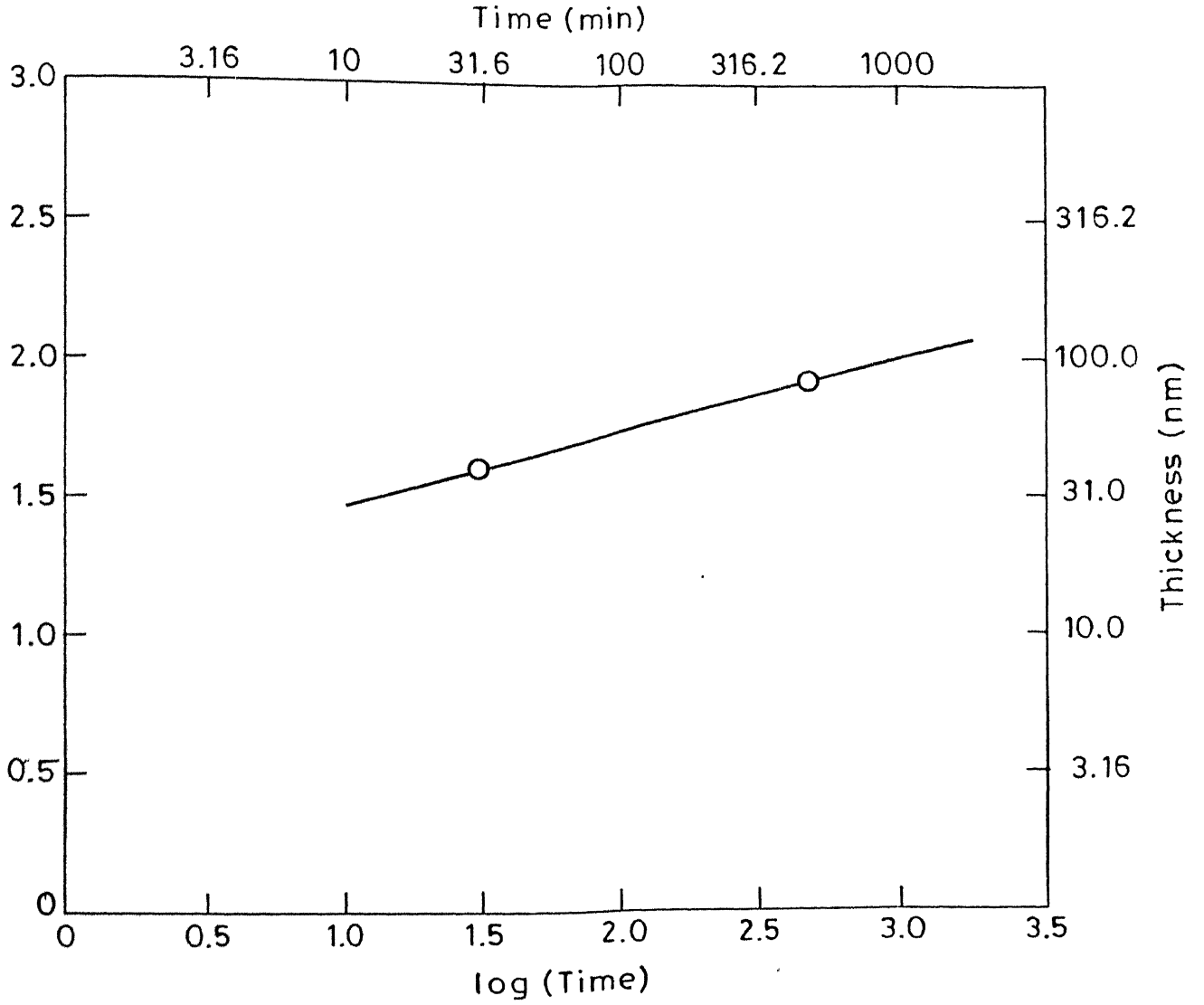

Fig. III.15 Plot of log (Thickness) vs log (Time) for a porosity of ~32% .

Table III.19

Grain size of the ZrO_2 coatings treated at 1250 °C

Coating thickness (nm)	Grain size (nm) after annealing at 1250 °C for 5 min.	30 min.	4 hrs.	8 hrs.
41	71.2	79.77	82.6	148.4
86	73.85	105.2	132.34	180.34
105	100.55	125.5	133.9	307.7
137	--	132.3	--	327.3

Table III.20

Values of 'n' for the two regions of the curves in Fig. III.16

Coating thickness (nm)	Slope of the straight line portions or value of 'n' Region 1	Region 2
41	0.04	0.83
86	0.148	0.466
105	0.077	1.20

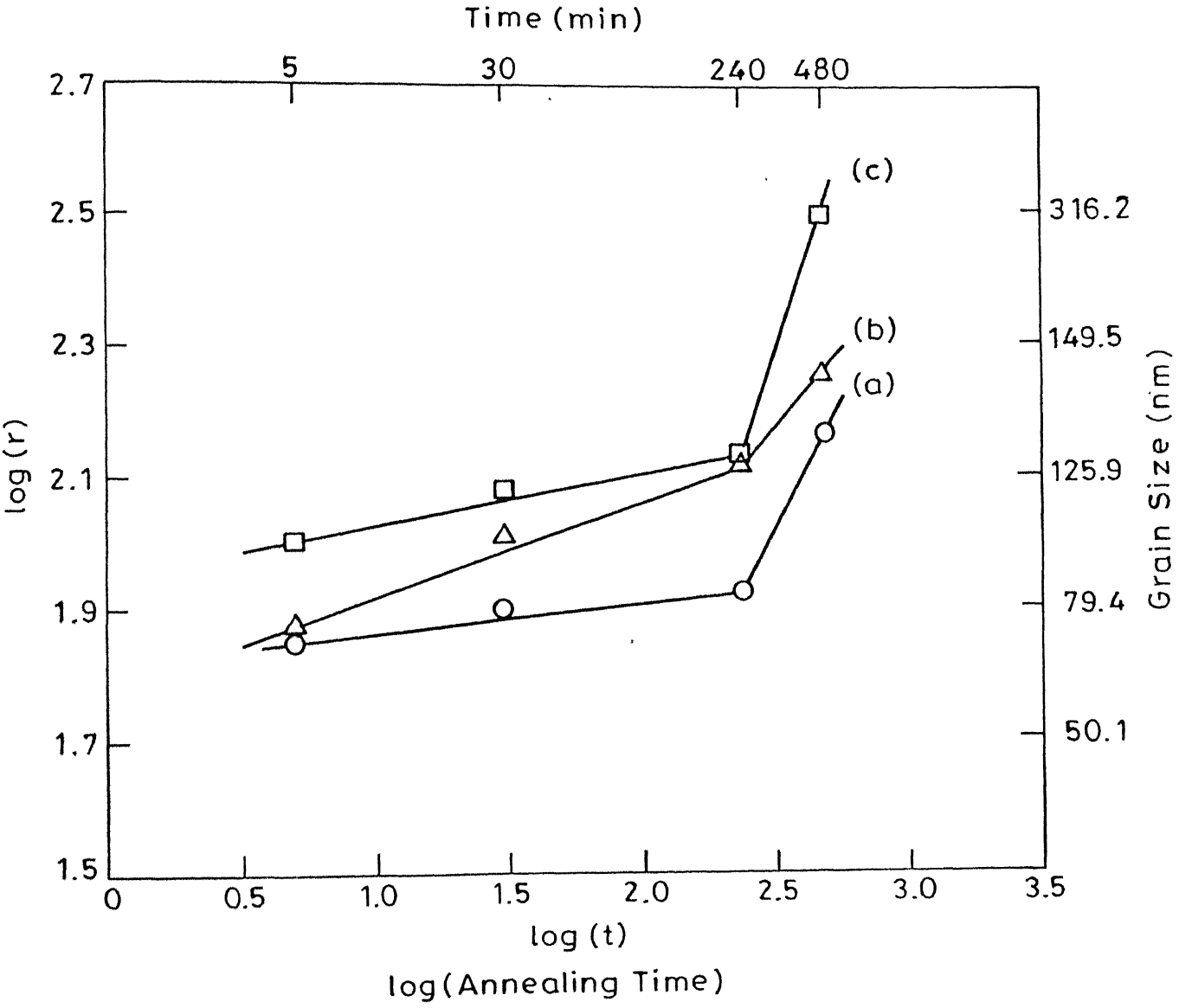

Fig. III.16 Variation of grain size with the annealing time for the coating thickness. (a) 41 nm (b) 86 nm (c) 105 nm.

occurs (Fig.III.11(g)). The slopes of the lines for different thickness coatings are given in Table III.20.

So it is evident that the growth law $d = k\,t^n$ is valid for only certain range for the coatings. The initial grain growth rate is small but later increases very rapidly. Curves 1 and 3 show more similar slopes than the curve 2. So from these we can say for the annealing times less than 4 hours the exponent in the growth law (n) has a value of 0.04-0.07.

III.7 Optical Band Gap Energy

We have shown in Fig. III.17 the actual recorded optical absorption spectra in the range of 200 nm - 900 nm for all the four different thicknesses of coatings. Transmittance Vs. wavelength spectra for the samples is also shown in Fig. III.18.

For $h\nu \ll E_g$ i.e. at 900 nm we have compared the absorptance for different thicknesses which is shown in Fig. III.19. It shows linear dependence on thickness as predicted by eqn. (5). This justifies the measured relative thicknesses of the films. Absorption coefficient at this wavelength is given by the slope of the line in Fig. III.19.

Figure III.20 shows the plot of $(Kh\nu)^2$ Vs.$h\nu$ for the energies near the band gap. Extrapolation to k = 0 yields an energy gap of 5.42 eV for the sample 4. Similar calculations are done on the other different thickness coatings and the values are given in the Table III.21.

The value of 5.16 eV is reported for the ZrO_2 films formed from CVD of organometallic compounds[6] and E_g = 5.12 eV[86] and 4.99 eV[90] are also reported. The value we have

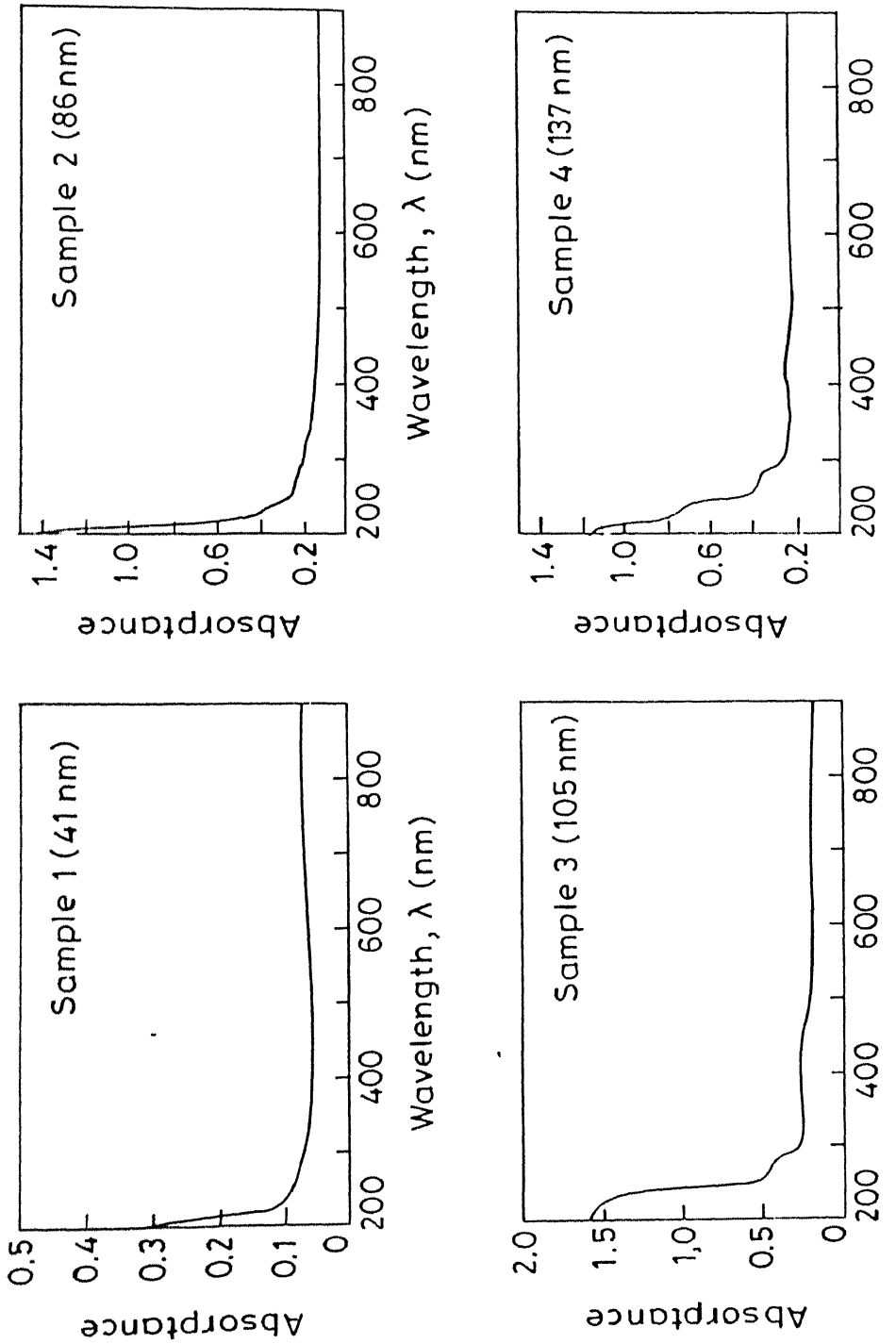

Fig. III.17 Optical absorptance of ZrO_2 coatings of different thicknesses.

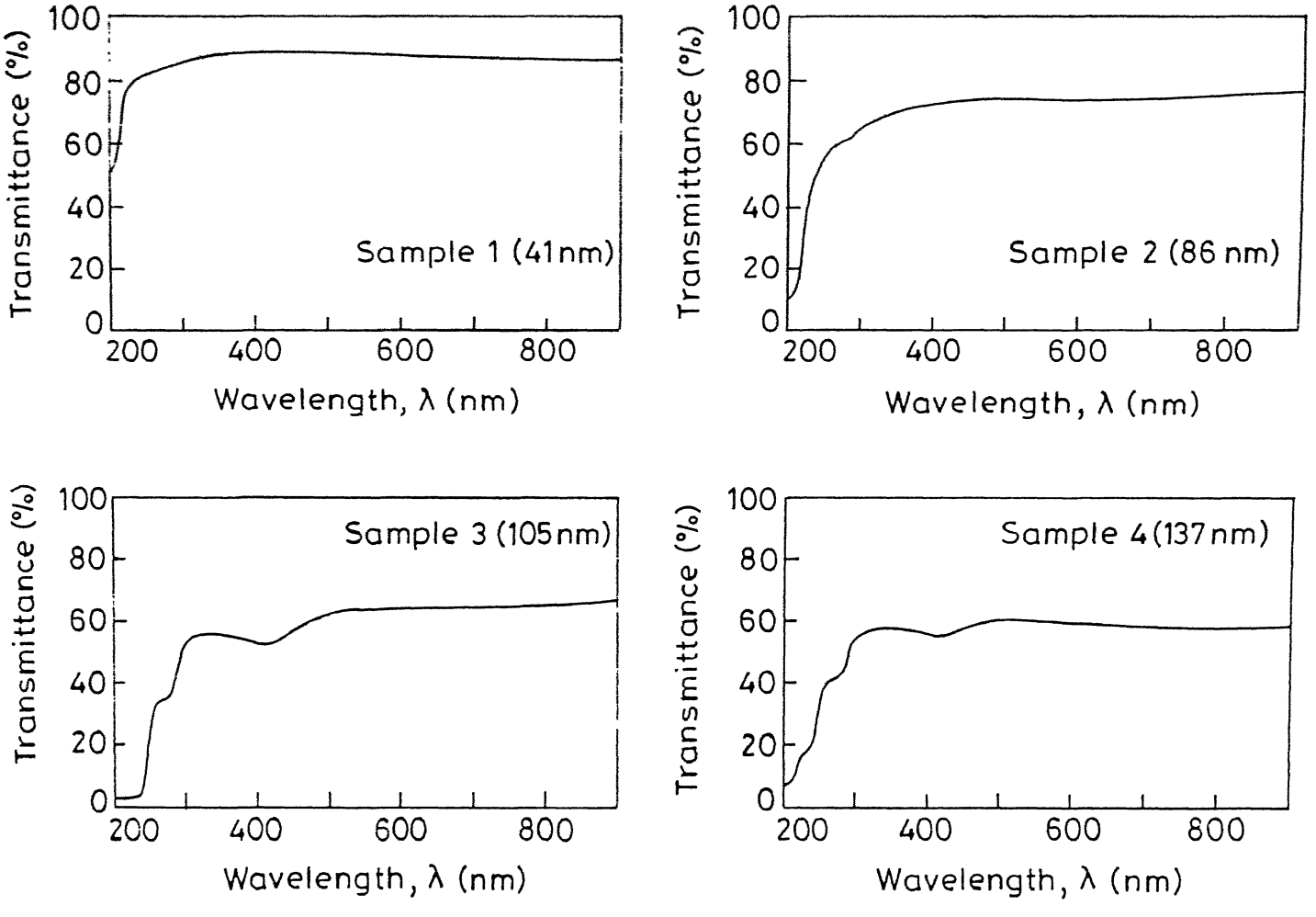

Fig. III.18 Optical transmittance of ZrO_2 coatings of different thicknesses.

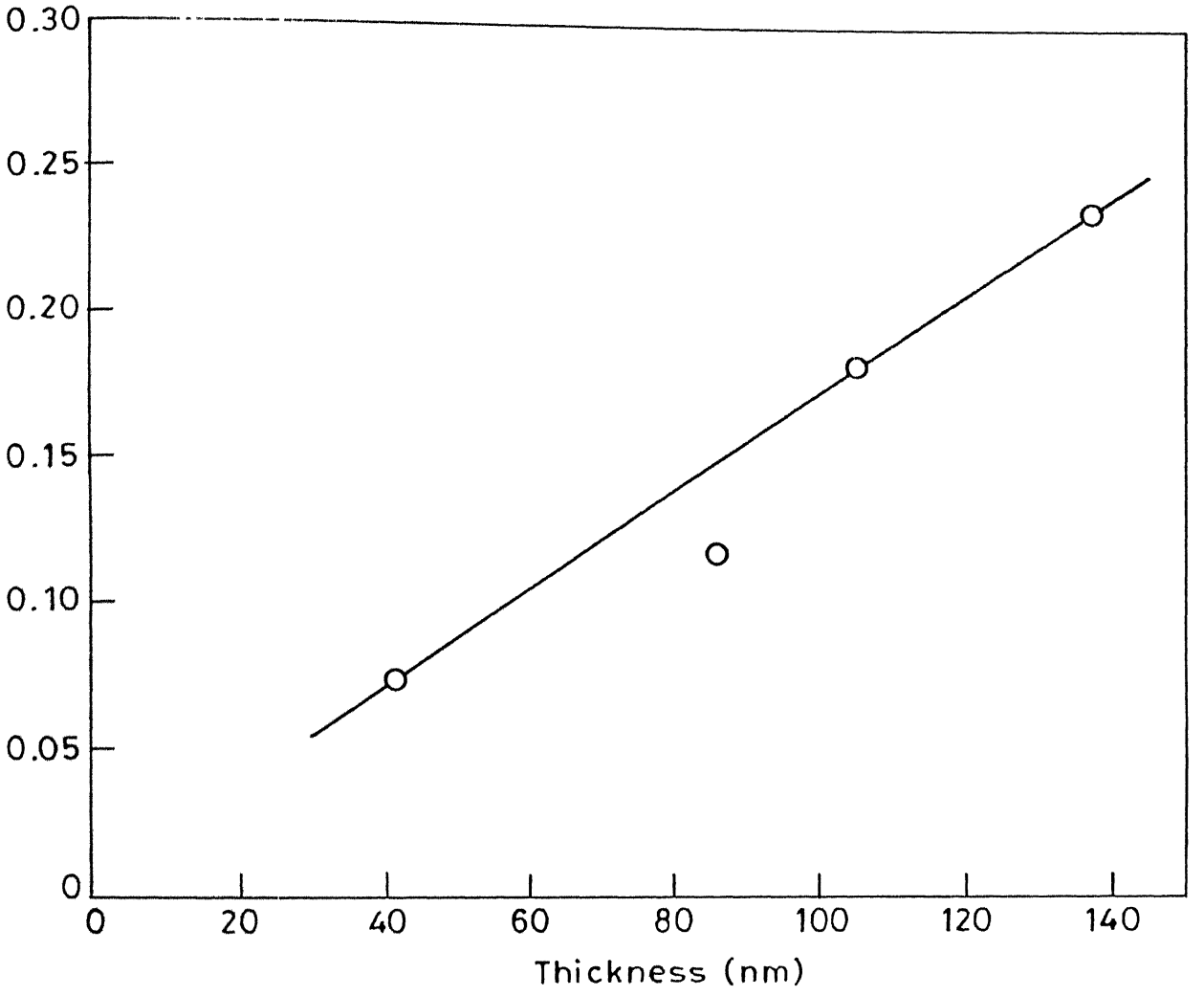

Fig. III.19 Variation of absorptance at 900nm for different thickness coatings.

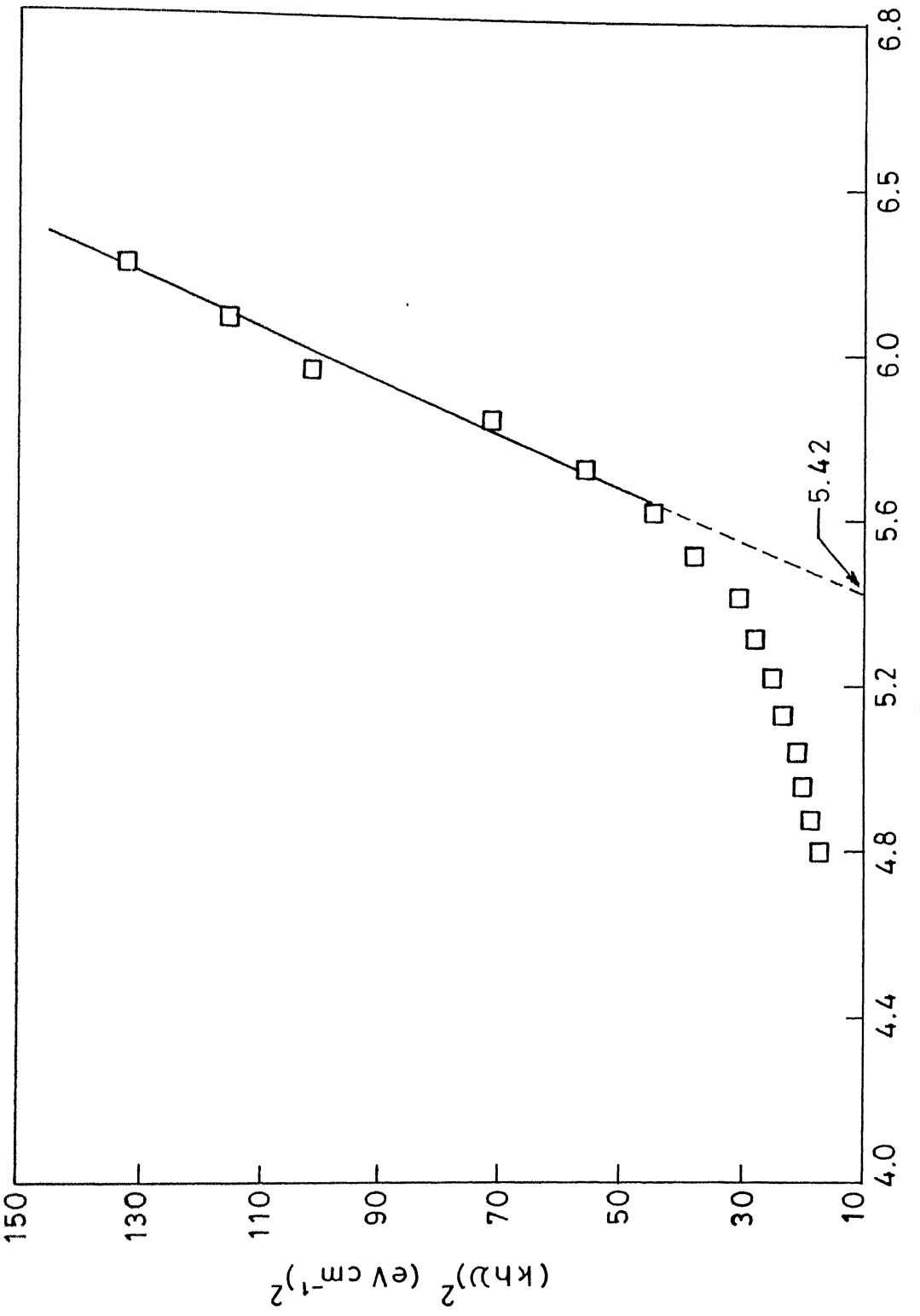

Fig.III.20 Plot of $(k\hbar\nu)^2$ vs $\hbar\nu$ for ZrO_2 coating of the thickness 137 nm.

Table III.21

Optical band gap energy values of the ZrO_2 coatings.

Sample No.	No. of times Coated	Band gap energy E_g (ev)
1	Once	5.72
2	Twice	5.71 ; 5.56
3	Thrice	5.08
4	Four times	5.42

Average Value = 5.498 ev.

obtained is in agreement with the previous values. There exists a correlation between the energy gap and the heat of formation per equivalent of the oxide as

$$E_{g+20\%} = \frac{2\,\Delta H_f}{\text{equiv.}}$$

where $\frac{H_f}{\text{equiv.}}$ is heat of formation per equivalent.

Taking $H_f = -64.5$ Kcal/equiv.[6], one gets

$$E_g = \frac{2\,\Delta H_f}{\text{equiv.}} = 2\left(-64.5\ \frac{\text{Kcal}}{\text{equiv.}}\right) = -5.59\text{eV}.$$

The value of 5.498 eV is within the 20% limit.

CHAPTER IV

CONCLUSIONS

1) It is found that DEA is more effective than DEG (for the same amounts) in preventing the precipitation of oxides in the zirconia sol, with the present experimental conditions and the chemicals used.

2) The molar ratio DEA/Zrnp = 0.74 is found to be optimum for preparing reasonably good films by dip coating method.

3) Multiple dipping gives thicker coatings and the thickness varies linearly with the number of dips for the same pulling speed.

4) The wetting of the sol on glass slides is better than that on sapphire substrates. It is illustrated by higher thickness coatings on glass slides than on sapphire substrate for equal number of dips.

5) The cracking of the films takes place with the rise of temperature and the extent of cracking increases with the thickness. The thermal stresses, phase transformation stresses (t-->m, compressive stresses due to volume expansion) and shrinkage stresses may be the reasons for the film to crack and form islands of higher thicknesses after the treatments at 1250°C.

6) The as deposited films are amorphous. On heating they transform to crystalline phases in the sequence amorphous-cubic - monoclinic. The bulk gel, on the other hand, displays an intermediate tetragonal phase ,the transformation sequence being amorphous - cubic - tetragonal - monoclinic. Absence of

tetragonal phase in the films is surprising because the tetragonal phase is expected to be more easily observed below a critical particle size and so should also be found in the film.

In the films, the cubic phase obtained after annealing at 450°C has a (200) texture. On annealing at 900°C the phase present is monoclinic with no texture. However a 1250°C treatment causes a (002) monoclinic texture to develop.

7) It is found that 8 mole % Y_2O_3 stabilizes the gel derived ZrO_2 tetragonal phase completely in contrast to the conventional methods, where still higher percentage is needed. The doping is easy and also effective and is achieved by using Yttrium nitrate salt.

8) The porosity development in thicker films is slower than that in thin films. Time for development of a given porosity varies as square of the thickness of the coating. This result indicates that the porosity development is controlled by diffusion along the thickness direction of the film.

9) The grain growth in the films at 1250°C follows the relation $d \propto t^{1/2}$ to certain range of annealing time and after that the exaggerated grain growth starts.

10) It is found that the sol gel prepared ZrO_2 films are direct band gap materials and the band gap is determined to be 5.498 ev, by optical absorption method. This value is much closer to the theoretical estimate than the values for zirconia films prepared by other routes.

REFERENCES

1) Metals Hand Book, ASM, Vol. 5, p. 533.

2) P.J. Martin, R.P. Netterfield, W.G. Sainty, "Modification of the Optical and Structural Properties of Dielectric ZrO_2 Films by Ion-Assisted Deposition", J. Appl. Phys. 55 (1984), 235-241.

3) R. Sivakumar, M. Srivastava, "Thermal Barrier Coatings by Plasma Spraying", DMRL, Hyderabad, Technical Report, May 1983.

4) S.K.Sim, Better Ceramics Through Chemistry II, MRS, Pittsburgh, Penn (1986) pp. 647.

5) S.M. Sim, P.Y. Chu, R.H. Krabill and D.E. Clark, "Chemically Derived Refractory Coatings", "Ultrastructure Processig of Advaced Ceramics",edited by J. D. Mackenzie, D.D. Ulrich, (John Wiley and Sons, Inc. 1988), p.995.

6) M. Balog; M. Schieber, "The Chemical Vapour Deposition and Characterization of ZrO_2 Films from Organometallic Compounds", Thin Solid Films, 47 (1977), 109-120.

7) K.V.S.R. Apparao, N.K. Sahoo, T.C. Bagchi, "Low Loss ZrO_2 Films for Optical Applications in the UV Region", Thin Solid Films, 129 (3-4), 1985, L71-73.

8) C.N. Panagopoulos, "Charge Storage in Anodic ZrO_2 Films", Mater. Lett. 1987, 5 (1-2) 31-4.

9) Akimune Yoshio, Ambe Satoshi, "Oxygen Sensor Element Having a Thin Layer of Stabilized Zirconia Stabilized on a Substrate. Patent Nissan Motor Co. Ltd. GB,2,087,569, 26 May 1982 Ceram. Abstracts 62 - 054443P (1983).

10) Kamata, Kii Chiro, Matsumato, "Y_2O_3, ZrO_2 and Stabilized ZrO_2 Films prepared by Chemical Vapour Deposition", Yogyo Kyokaishi 1982, 90(1) 46-7.

11) D. Nguyen, M. Van Roode, W.Sze, "Zirconia Coatings Prepared by Spray Pyrolysis", J. Can. Ceram. Soc. 1984, 53, 34-8 (Ceramic Abstracts 1985).

12) Krivosheev, N.V. Zapleshko, N.N. Fedorov.Izv. Akad. Nauk. SSSR, Neorg. Mater. 1983, 19(6), 916-19 (Russian) (Ceramic Abstract 1984).

13) P.J. Martin, R.P. Netterfield, W.G. Sainty, "Ion Assisted Deposition of Bulk Like ZrO_2 Films", Appl.Phys. Lett. 1983, 43(8), 711-13.

14) Rolls-Royce Ltd. US. Patent, "Forming (ZrO_2 based) Coating by Hot Isostatic Compaction" (Ceramic Abstract 1985).

15) M. Croset, J.P. Schnell and G. Velasco, J. Siejka, "Composition, Structure, and AC Conductivity of rf. Sputtered Calcia - Stabilized Zirconia Thin Films, J. Appl. Phys. 48(2),775-80 (1977).

16) Siemens, A. Paul, "Mechanical And Physical Properties of Plasma Sprayed Stabilized ZrO_2". Ceram. Engg. Sci. Proc. (1983), 4(9-10) 828-40 (Ceramic Abstract 1984).

17) Miller, A. Robert, Garlick,G. Ralph, "Phase Distribution in Plasma Sprayed ZrO_2 - Y_2O_3", Am. Ceram. Soc. Bull. 1983, 62(12), 1355-8 (Ceramic Abstract 1984).

18) Shankar, N. Ravi, Berndt, "Phase Analysis of Plasma Sprayed Zirconia Yttria Coatigs", Ceram. Engg. Sci. Proc. 1983, 4 (9-10) 784-91 (Ceramic Abstract 1984).

19) R. Mc. Pherson, R. Houghton, "Yttria - Partially Stabilized Zirconia Plasma-Sprayed Coatings", J. Aust.Ceram. Soc.1984,

20(2) 235.

20) P. Boch, P. Fauchais, D. Lombard: "Plasma Sprayed Zirconia Coatings", Advances in Ceramics, 1984, 12, 488-502 (Ceramic Abstract 1985, 64 (7-8) 64-05996(B).

21) Shankar, N. Ravi, Berndt, "Failure and Acoustic Emission - Response of Plasma- Sprayed ZrO_2 - 8wt% Y_2O_3 Coatings", Ceramic. Engg. Sci. Proc. 1982, 3 (9-10) 772-92.

22) "Thermal Stability of Plasma-Sprayed ZrO_2 Coatings as Related to Substrate Selection", Am. Ceram. Soc. Bull. 1985, 64(9), 1268-71.

23) Fischman, S. Gary, C.H. Chen, J.M. Rigsbee, "Character of Laser Glazed, Plasma Sprayed ZrO_2 Coatings on Stainless Steel Substrate", Ceram. Eg. Sci. Proc. 1985, 6 (7-8) 908-18 (CA 6500895A).

24) Padovan, Chung, Ceram. Engg. Sci. Proc. 87, 8 (7-8) 572-82.

25) Dongare; M.K. Sinha, "Low Temperature Preparation of Stabilized ZrO_2", J. Mater. Sci., 1984, 19(1), 49-56.

26) C. Panagopoulos, "Structural Study of Anodic ZrO_2 Films", Mater. Lett. 1985, 3(9-10) 393-5.

27) Sankar, Dantale et al., "Materials Modification annd Growth using Ion Beam", Symposium Anaheim, CA, USA, 21-23 APR,1987.

28) M. Morita, H. Fukumoto, T. Imura and Y. Osaka, M. Ichihara, "Growth of Crystalline Zirconium Dioxide Films on Silicon", J. Appl. Physics, 1985, 58(6), 2407-9.

29) L.C. Klein, "Sol-gel Processing of Silicates", Ann. Rev. Mater. Sci., 1985, 15, 225-48.

30) W.Geffcken and E.Berger, Dtsch., Reichspatent 736 411 (1939), Jenaer Glaswerk Schott and Gen., Jenna, GDR

(Obtained from Ref. (34)).

31) H. Schroeder, "Oxide Layers Deposited from Organic Solutions", Physics of Thin Films, Vol. 5.Edited by Georg Hass and R.E.Thun (Academic Press, New York, London),1969, pp. 87.

32) J. Langmuir, J. Am. Chem. Soc. 39, 1848 (1917) (Obtained from Ref. (31)).

33) K.B. Blodgett, J. Am. Chem. Soc. 57, 1007 (1935) (Obtained from Ref. (31)).

34) H.Dislich and P.Hinnz, "History and Principles of the Sol-gel Process, and Some New Multicomponent Oxide Coatings", J. Non. Cryst. Solids, 48 (1982), 11-16.

35) H. Dislich, Angew, Chem. Int. Ed. Engl.10(6),(1971), 363 (Obtained from Ref. (34)).

36) H. Dislich, E. Hussmann, Thin Solid Films, "Amorphous and Crystalline Dip Coatings obtained from Organometallic Solutions; Procedures, Chemical Processes and Products", 77 (1981), 129-139.

37) D.R. Uhlmann, G.P.Rajendra, "Coatings: The Land of Opportunity for Sol-gel Technology", Ultra Structure Processing of Advanced Ceramics. Edited by J.D. Mackenzie, D.D.Ulrich (John Wiley Interscience,1988), p.241.

38) R.B. Pettit, C.J. Brinker, Proc. SPIE, Opt. Mater. Tech. Engg., Eft. Solar. Energy, Convocation IV, 562,256 (1985).

39) M. Guglielmi, A. Maddalena, "Coatings of Glass Fibres for Cement Composites by the Sol-gel Method", J. Mater.Sci. Lett. 4,(1985), 123-124.

40) A. Maddalena, M. Guglielmi, V.Gottardi, A. Raccanelli, "Interactions with Portland Cement Paste of Glass Fibres

Coated by the Sol-Gel Method", J. Non-Cryst Solids,82, (1986), 356.

41) W. Beier, A.A. Goktas and G.H. Frischat, "Thin SiO_2-TiO_2-ZrO_2 Films from Alkoxide Solutions", J. Non-Cryst. Solids, 100 (1988), 531-537.

42) V.C. Haskell, J.L. Hecht, U.S. Patent, 3,857, 723 (1974) (Ceramic Abstract 1975).

43) A. Makishma, M. Asami, K. Wada, "Preparation of CeO_2-TiO_2 Coatings by the Sol-gel Process", J. Non-Cryst. Solids,100 (1988) 321.

44) I. Strawbridge and P.F.James, "Thin Silica Films Prepared by Dip Coating", J. Non-Cryst. Solids,82 (1986), 366-372.

45) I. Strawbridge and P.F. James, "The Factors Affecting the Thickness of Sol-gel Derived Silica Coatings Prepared by Dipping", J. Non-Cryst. Solids,86 (1986), 381-393.

46) Yasutaka Takahashi, Yoshihiri Matsuoka, "Dip Coatings of TiO_2 Films using a Sol Derived from $Ti(O\text{-}i\text{-}Pr)_4$ - Diethanolamie - H_2O, i-PrOH System", J. Mater. Science, 23(1988), 2259-2266.

47) B.E. Yoldas, Appl. Optics, 21(1982), 2960.

48) Ezoe Masanobu, Kato Etsuro, "Fabrication of Oriented Polycrystalline Titania Films by Sol-gel Process", Yogyo Kyokaishi 1987, 95 (12) 1207-12 (Japanese), Ceramic Abstract, 1989.

49) R.A, Lipeles, N.A.Ives, and M.S. Leung, "Sol-gel Processing of Lead Zirconate Titanate Films", Science of Ceramic Chemical Processinng (Wiley Interscience, 1986),pp. 320.

50) D. Kundu, Prasanta Kumar, D. Ganguli, "Alkoxide-Derived Amorphous ZrO_2 Coatings", Thin Solid Films, 163 (1988), 273-278.

51) K.P. Speck, H.S. W. Hu, M. E. Sherwin and R.S. Potember, "Vanadium Dioxide Films Grown from Vanadium Tetra Isopropoxide by the Sol-gel Process", Thin Solid Films,165 (1988), 317-322.

52) H.C. Ling, M.F. Yan and W.W. Rhodes, "Science of Ceramic Chemical Processing", edited by L.L. Hennch and D.R. Ulrich (Wiley, New York, 1986), pp. 285.

53) J. Martinsen, "Better Ceramics through Chemistry edited by C.J. Brinker, D.E. Glarck and D.R. Ulrich, (North Holland, New York), 1984.

54) M.F. Gruninger, J.B. Wachtman, MRS.New York, (1986), p. 823.

55) M. Nogami and Y. Moriya, Yogyo-Kyokaishi, 85 (1977), 448 (Ceramic Abstract 1978).

56) F.Bel Hadj, R. Sempere and J. Phalippou, "Study of Thin Solid Films Elaborated by DIP Coating", J. Non-Cryst., Solids. 82(1986), 417-425.

57) C. Guizard, N. Cygankiewicz, A. Larbot and L. Cot, "Sol-gel Transition in Zirconıa Systems using Physical and Chemical Processes", J. Non.Cryst. Solids,82 (1986), 86-91.

58) J.C. Debsikdar, "Transparent Zirconia Gel-Monolith from Zircoium Alkoxide", J. Non. Cryst. Solids 86 (1986) 231-240.

59) J.C.Debskidar, "Thermal Evolution of Alkoxy-Derived Glass-Like Transparent Zirconia Gel", J. Non. Cryst. Solıds,87 (1986), 343-349.

60) R.C.Garvie, "The Occurrence of Metastable Tetragonal Zirconia as a Crystallite Size Effect", J.Phys. Chem.69

(1965) 1238.

61) I.J. Mc Colm, "Ceramic Science for Materials Technologists" (Leonard Hill, New York), 1983, pp. 272.

62) E.D. Whitney, "Kinetic and Mechanisms of the Trasition of Metastable Tetragonal to Monoclinic Zirconia", Faraday Soc. 61(9), (1965), p. 199.

63) D. Kundu, D. Ganguli, "Monolithic Zirconia Gels from Metal-Organic Solutions", J. Mater. Sci. Lett. 5 (1986),293 295.

64) D. Ganguli, D. Kundu, "Preparation of Amorphous ZrO_2 Coatings from Metal-Organic Solutions", J. Mater. Science Letters., 3 (1984),pp. 503-504.

65) N.A. Genkina, P. Pavlov, "Structure of ZrO_2 Films Prepared from Zirconia Acetylacetonate", Izv. Akad. Nauk. SSSR. Neorg. Mater. 1983,19(7), 1114-7 (Russian) (Ceramic Abstract 64-01579A)).

66) Takahashi, Yasutaka, Niwa, Katsukiro Kobayashi, Keisuke,"Dip Coating of Zirconia and Mixed Zirconia Films", Yogyo Kyokaishi, 1987, 95(10), 942-8 (Japanese), Ceramic Abstracts, 68-01246A (1989).

67) Toghe Noboru, Matsuda Atsunori, Minami Tsutomu, Chem. Express, 1987,2(3), 141-4 (CA 67-03356A), (1988).

68) Ezoe Masanobu, Murase Yoshio, Daimon Keiji, "Formation and Thermal Change of Monoclinic Zirconia (m-ZrO_2) Polycrystalline Thin Films by Sol-gel Process", Yogyo Kyokaishi, 1986, 94(8),823-6 (Japanese) (CA 67-06737A (1988)).

69) C.J.Brinker, A.J. Hurd and K.J. Ward, "Fundamentals of Sol-gel Thin-Film Formations", Ultrastructure Processing of Advanced Ceramics, Edited by J.D. Mackenzie,D.R.Ulrich

(John Wiley and Sins), 1988, p. 223.

70) D.I. Butts, W.C.La Course, S.Kim, "Influence of Sol and Substrate Chemistry on the Formatıon of Sol-gel Derived Coatings", J. Non-Cryst. Solids, 100 (1988), 514-518.

71) L. Landau and Bevich, Physicochim. URSS, 17 (1942), 42 (From Ref. (45)).

72) F. Orgaz, F. Capel, "A Semi-empirical Model for Coating Flat Glass by Dipping into Metal-organic Solutions", J. Mater. Sci. 22 (1987), 1291-1294.

73) C.C. Yang, J.Y. Josefowicz and L. Alexandru, Thin Solid Films, 74 (1980) 117 (From Ref. (45)).

74) H. Schroeder, Opt. Acta,9, 249 (1962).

75) B.E.Yoldas, "Surface Roughness of Optical Oxıde Coatings Deposited from Solutions and the Morphological Effect of Different Deposition Methods", Mat.Resc. Soc. Symp. Proc., Vol. 47 (1985), p. 107.

76) Sumio Sakka, "Glasses and Glass-Ceramics through the Sol-gel Process", "Advanced Ceramics II" edited by Shigeyuki Somiya, (Elsevier Applied Science, London and New York), 1986, p. 163.

77) Dislich, "Glassy and Crystalline Systems from Gels Chemical Basis and Technnical Applications, J. Non. Cryst. Solids,57 (1983), 371-388.

78) J.D.Mackenzie, "Applications of the Sol-gel Processes", J. Non.Cryst. Solids, 100 (1988) p.62.

79) B.E. Yoldas, "Modification of Oxides by Polymerzation Process", Ultrastructure Processing of Ceramics, Glasses and Compsotes (Wiley - Interscience, 1984), pp. 60.

80) S. Tolanski,"Multiple Beam Interfer ometry of Surfaces and

Films", (Oxford,1949), p. 10.

81) Mirau Interference Equipment,Carl Zeiss Companny, Manual.

82) Robert T. DeHoff, Fredenick N. Rhines, Quantitative Microscopy (McGraw Hill Book Co., 1968), pp. 72.

83) W. Rostoker, J.R. Dvorak, "Interpretation of Metallographic Structures", 2nd edition (Academic Press, 1977), p. 226.

84) A.I. Vogel, "Quantitative Inorganic Analysis" (ELBS and Longmans Green and Co., 1961), p. 738.

85) J.J. Pankove, "Optical Processes in Semiconductors", (Prentice Hall Engle Wood Cliffs) 1971.

86) R.N. Tauber,A. C.Dumbri and R.E. Caffrey, J. Electrochem. Soc. 118 (1971), 747. (From Ref. (6)).

87) R. Tomac, "ASTM Data", Private Communication.

88) "Powder Diffraction File", Published by JCPDS Set 5-10(7-063).

89) Gerald Katz, "X-ray Diffraction Powder Pattern of Metastable Cubic Zirconia", J. Am. Ceram. Soc. 54(10), 531 (1971).

90) J.G. Bendoraitis and R.E. Solomon, J. Phys. Chem. 69 (1965), 3665 (From Ref.(6)).